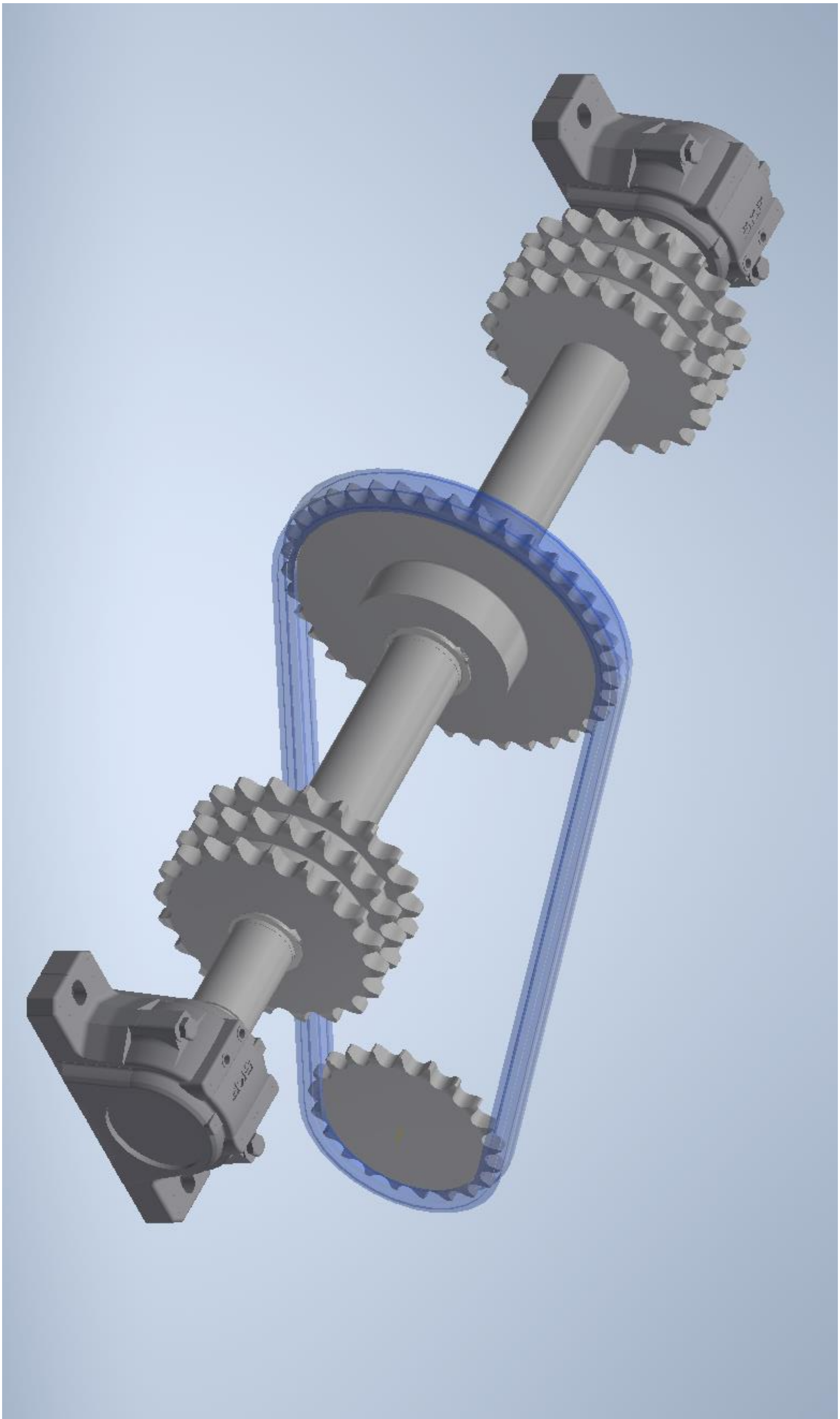

ME22007 Sub-assembly Design Exercise:

Shaft design of a transmission shaft sub-assembly of a Forklift

Written by: Elliot Routier, Caleb Otto Sumner-Box, Ilhan Shahril and Vedasri Tirumala

Table of Contents

Summary

The design for our forklift's transmission shaft focuses on optimising durability, cost-efficiency, and sustainability. Through iterative analysis, materials like Al-7068 and Stainless-Steel AM 355 were considered as well as different power transmission components, in terms of strength, torsional properties, and manufacturing costs while meeting the operational requirement of lifting 1-tonne stone blocks in harsh conditions.

1 Introduction

The University of Bath is exploring low-carbon materials such as natural stone blocks to reduce the environmental impact of concrete. Since there is a long history of stone quarrying in Bath, it is being investigated to reduce carbon footprint. A new forklift design, using electric motors and a novel transmission shaft, is being developed to extract the stone.

The transmission shaft design focuses on reducing material carbon footprint, cost-effectiveness, and durability under tough conditions. It needs to handle 1-tonne stone blocks, operate at 30 rpm, and last 12 hours a day for 10 years. Vibration is minimised by securely positioning components, and stress analysis is done using torque, shear force, and bending moment diagrams. An iterative design process ensures the shaft can handle the anticipated load, and CAD drawings guide the final production.

2 Design Options

Different areas were researched to make sure the shaft was going to meet the requirements in the brief, producing 4 initial design options. Different areas were then researched to make sure the shaft was going to meet the requirements listed in the brief without failure.

2.1 Initial Analysis

The sub-assembly contains a shaft, a driven sprocket that transmits the torque from the motor to the shaft, two bearings supporting the shaft, two sprockets transmitting the torque from the shaft to the forklifting chain. A drawing of the design can be seen in *Figure 1*.

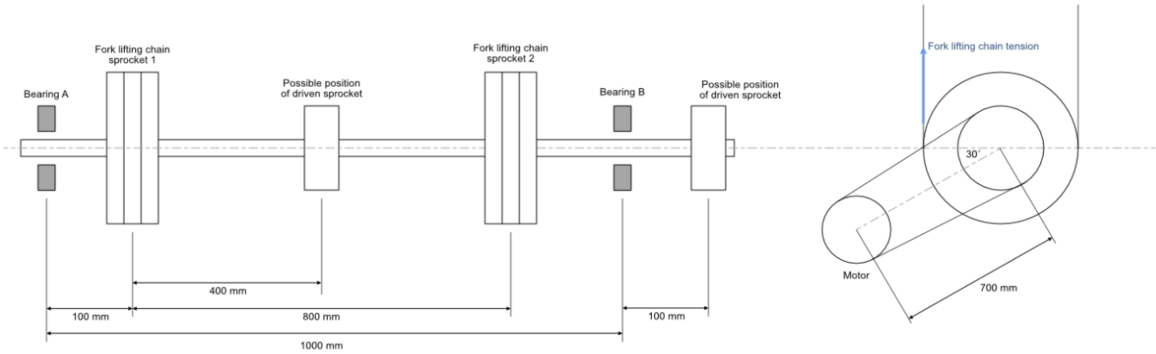

Figure 1 - Layout for shaft and transmission components. The two given driven sprocket locations are shown.

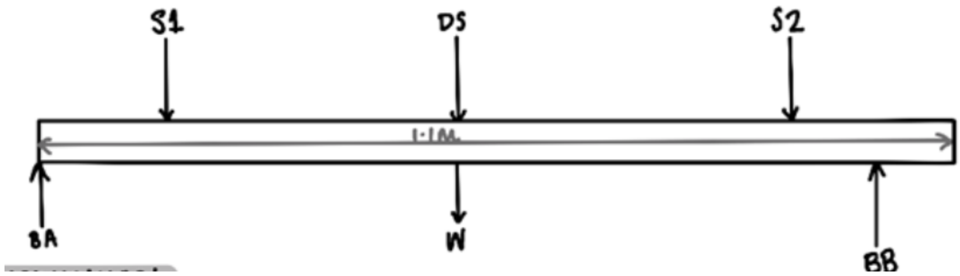

Figure 2 - FBD of Motor Option A

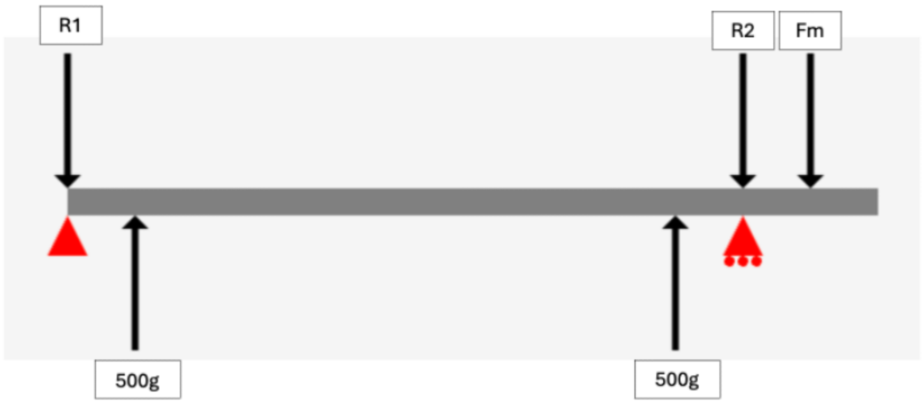

Figure 3 - FBD of Motor Option B

To differentiate the design options to cover a wide range of design metrics, initial design constraints were set for each design to evaluate the feasibility of the final design.

- Design Option 1:
  - Motor Option A, with driven sprocket located equidistant to the two fork sprockets
  - Maximum of 75mm shaft diameter

- Design Option 2:
  - Motor Option A, with driven sprocket located equidistant to the two fork sprockets

- Minimum of 75mm shaft diameter

- Design Option 3:
  - Motor Option B, with driven sprocket located by the very end of the shaft
  - Maximum 75mm shaft diameter

- Design Option 4:
  - Motor Option A, with driven sprocket located equidistant to the two fork sprockets
  - Minimum 75mm shaft diameter

Through the Iterations detailed in the sections below, these some of these initial constraints were deemed to be unfeasible for shaft design, allowing us to narrow down the essential design metrics used in the final design.

2.2 Design option 1

Design option 1 was explored by Elliot Routier with the driven sprocket in the middle of the shaft and the motor angle vertically down. Had the shaft been inclined at 30 degrees to the horizontal as detailed in the brief, the forces acting on the shaft would be a lot greater from the introduction of horizontal forces.

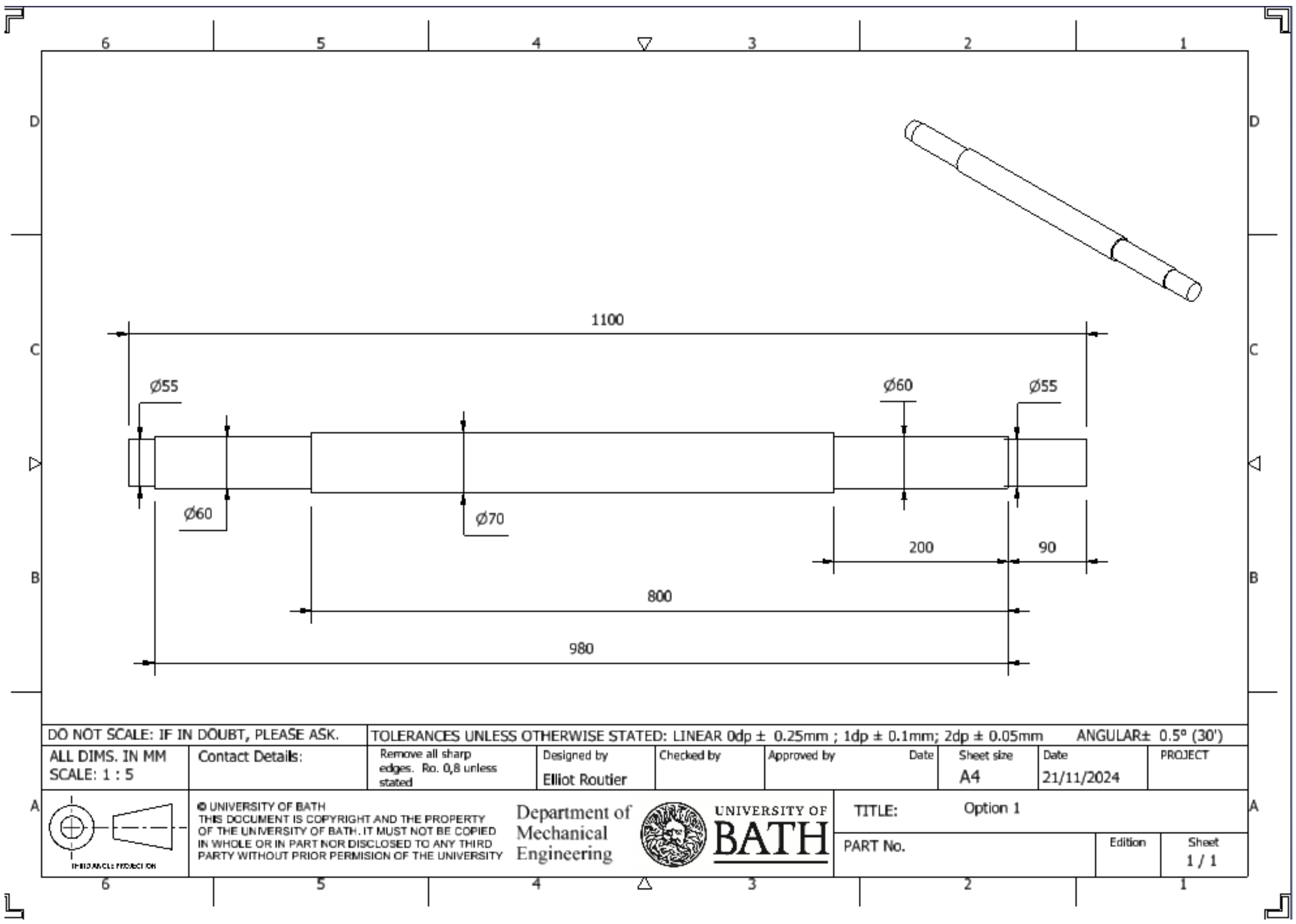

Figure 4 – Drawing of option 1 presenting principal dimensions.

2.1.1 Failure calculations

The failure calculations, tabulated in *Appendix 1*, show a total of 5 iterations that slowly improve the percentage failure. The appendix details all the changes, initial assumptions, geometries and calculations. In the final iteration, a stepped shaft ranging from 55 to 70 mm in diameter was used with Al 7068 as the material and an updated design factor of 7.

The following graphs show the bending moments and torques applied on the shaft for the final iteration:

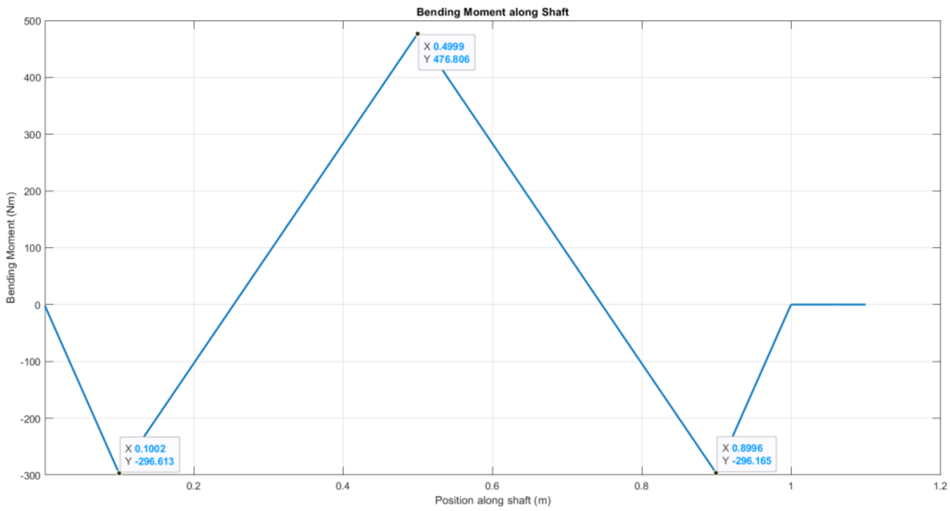

Figure 5 - Shows the bending moments along the shaft at the key nodes.

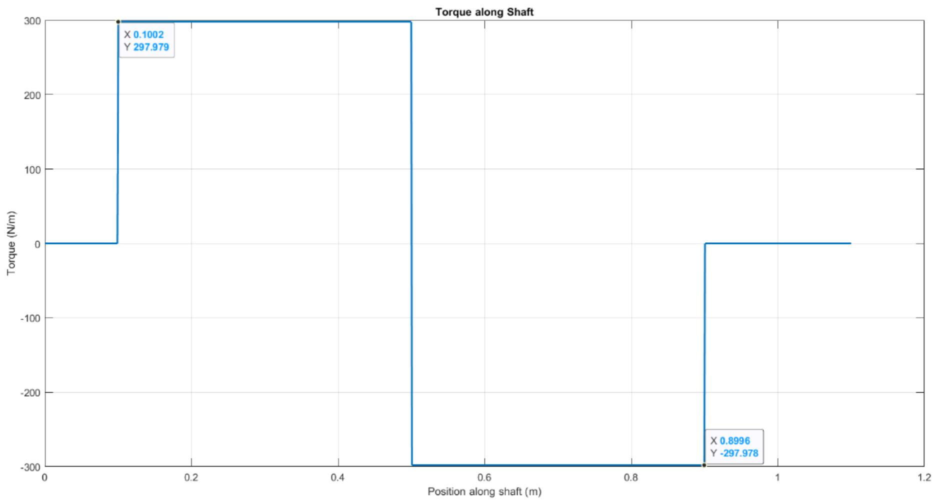

Figure 6 - Shows the torque applied along the shaft at key nodes.

2.2.2 Power Transmission

To satisfy the power requirements of a forklift, a chain drive transmission was selected where the chain selected was a 16B-1, the driving sprocket was a RN16B1Z25B, and the driven sprocket was a RN16B1Z38B.

2.2.3 Material Selection

7 different materials were compared and ranked based on their stiffness, torsional stiffness and torsional strength relative to their density. From best to worst, the materials rank:

1. Tungsten Carbide-Cobalt 84.02% WC
2. Carbon Steel AISI 1080
3. Stainless Steel AM 355
4. Al 7068
5. 4130 Steel (Low Alloy Steel)
6. Banana Fiber
7. Ni-Ti45 (Nitinol)

For reasons covered in the next section (manufacturing), the material selected for the shaft was Al 7068.

2.2.4 Manufacturing

The specific energy of a material directly contributes to the cost of manufacturing. As such, the Al 7068 was selected as it has the lowest specific energy, even though it didn't rank the best in terms of stiffness, torsional stiffness and torsional strength. A manufacturing cost for this shaft amounts to £2.27. The 5-kW lathe is used for the turning operations.

2.2.5 Bearings

For a basic static load rating of 2.97 kN on the bearing, the bearing selected was the 60/710 MA single row deep groove ball bearing.

2.2.6 Keys, keyways and key seats

3 keys are required on design option 1 to transmit the torque. 2 of these keys are 18 x 11 mm, the third key has dimensions 20 x 12 mm with key seat and keyway dimensions determined from *Table 7*. The key lengths were found to be 45 mm and 36 mm respectively from *Equation 2*.

2.2.7 Circlips

In total, 4 circlips were used for locating the sprockets. Two of these circlips were the DIN 471 DI 400 AA 70 and the other two circlips were the DIN 471 DI400 AA 60, selected from the Cirteq circlip catalogue.

2.3 Design option 2

Design option 2 was designed by Caleb Otto Sumner-Box, like design 1 the driven sprocket was in the middle of the shaft and the motor was angled vertically down.

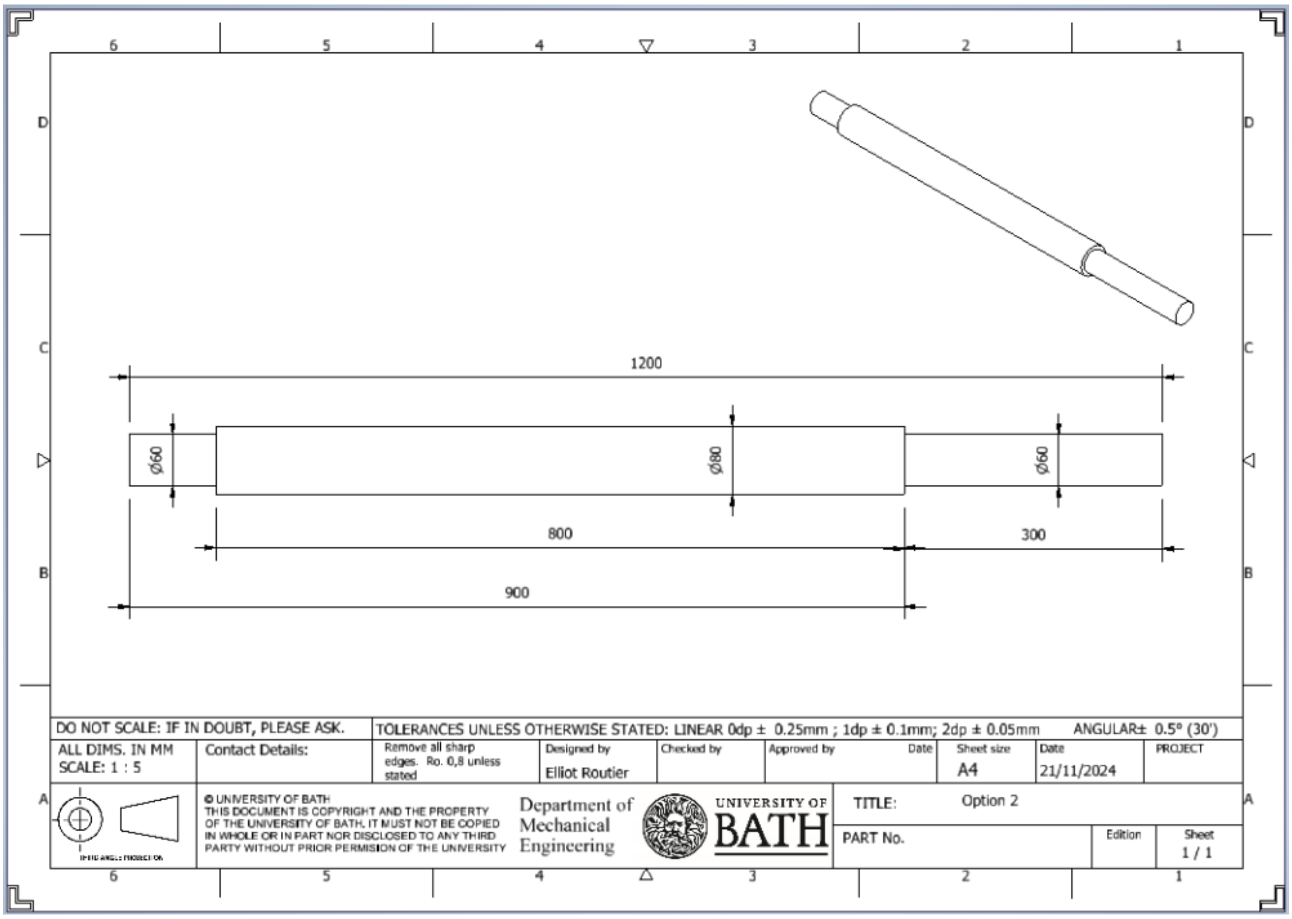

Figure 7 – Principal dimensions drawing for option 2.

2.3.1 Failure calculations

Appendix 2 shows a total of 3 iterations that slowly improve the percentage failure.

In the final iteration a stepped shaft ranging from 55mm to 80mm was used with 4130 Steel. The material yield strength was 700MPa and the design factor was 4.05.

The following graphs show the bending moments and torques applied on the shaft for the final iteration:

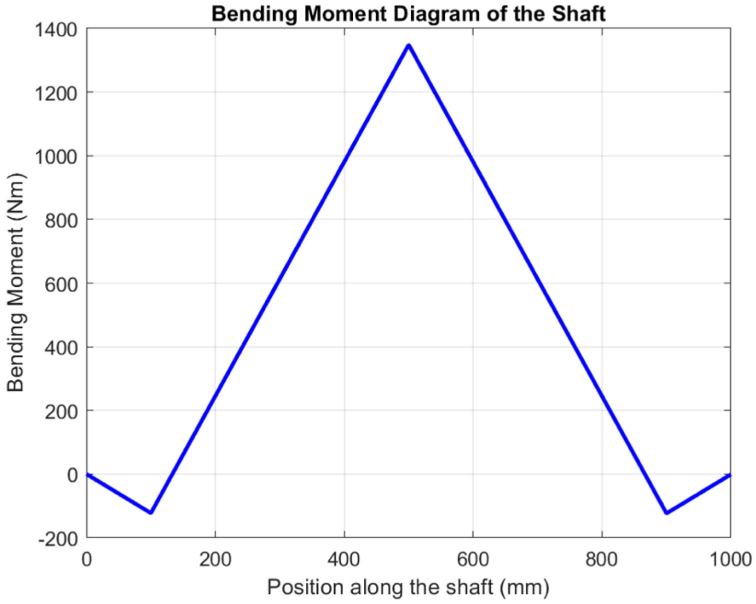

Figure 8 – Option 2 BM Diagram

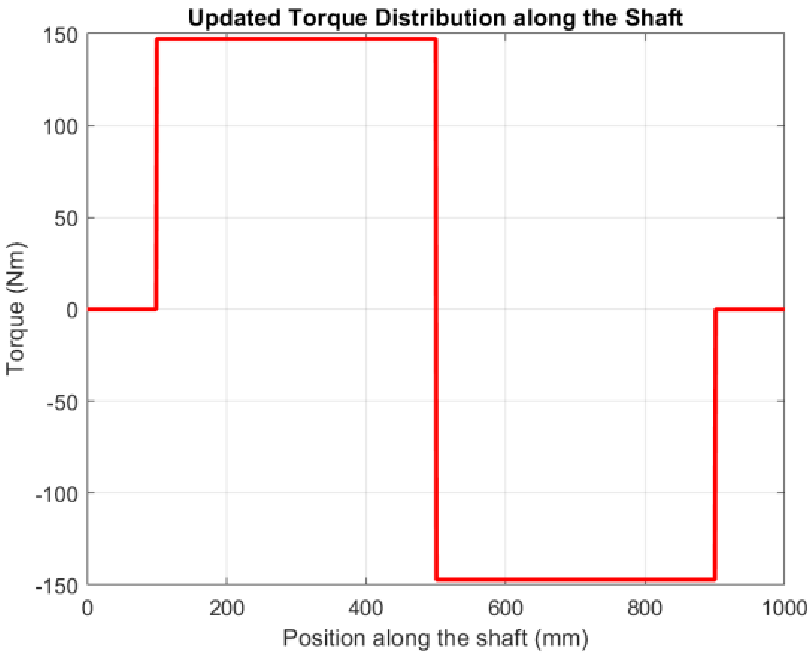

Figure 9 – Option 2 Torque Diagram

2.3.2 Power Transmission

To satisfy the power requirements of a forklift, a chain drive transmission was selected where the chain selected was a 16B-1, the driving sprocket was a RN16B1Z21B, and the driven sprocket was a RN16B1Z38B.

2.3.3 Material Selection

7 different materials were compared and ranked based on their stiffness, torsional stiffness and torsional strength relative to their density. From best to worst, the materials rank:

1. Tungsten Carbide-Cobalt 84.02% WC
2. Carbon Steel AISI 1080
3. Stainless Steel AM 355
4. Al 7068
5. 4130 Steel (Low Alloy Steel)
6. Silicon
7. Polythene fiber

2.3.4 Manufacturing

For reasons justified in *Appendix 2*, 4130 Steel was used for option 2. A manufacturing cost for this shaft amounts to £13.11. This cost is significantly higher than option 1. The 30-kW lathe is used for the turning operations involved to manufacture the shaft.

2.3.5 Bearings

For a basic static load rating of 1.227 kN, the bearing selected was the 61910 MA single row deep groove ball bearing.

2.3.6 Keys, keyways and key seats

3 keys are required on design option 2 to transmit the torque. 2 of these keys are 20 x 12 mm, the third key has dimensions 20 x 12 mm with key seat and keyway dimensions specified in *Table 7*. The key lengths were found to be 45 mm and 36 mm respectively from *Equation 2*.

2.3.7 Circlips

In total, 4 circlips were used for locating the sprockets. Two of these circlips were the DIN 471 DI 400 AA 75 and the other two circlips were the DIN 471 DI400 AA 55. Selected from the Cirteq circlip catalogue in *Figure 26*

2.4 Design option 3

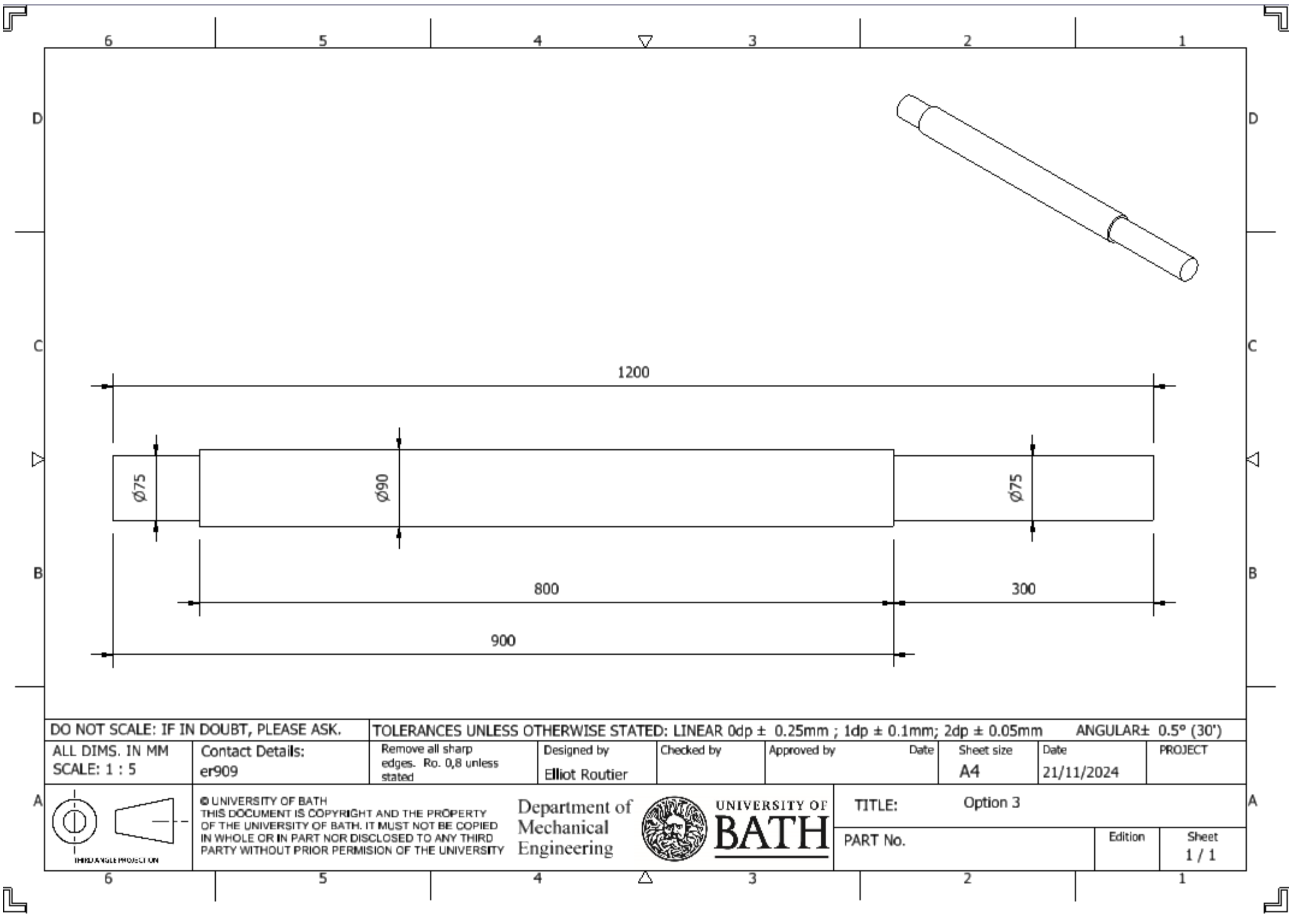

Figure 10 – Basic drawing of the principal dimensions of option 3

2.4.1 Failure calculations

Starting with an initial shaft design, as seen in *Appendix 3*, conditions for failure were calculated along each node of importance. In the final Iteration, the shaft diameter which varies from 90mm – 75mm, consisting of solid *4130 Steel (Low Alloy Steel)*, features a yield strength of 460 MPa as well as a design factor of 5.46.

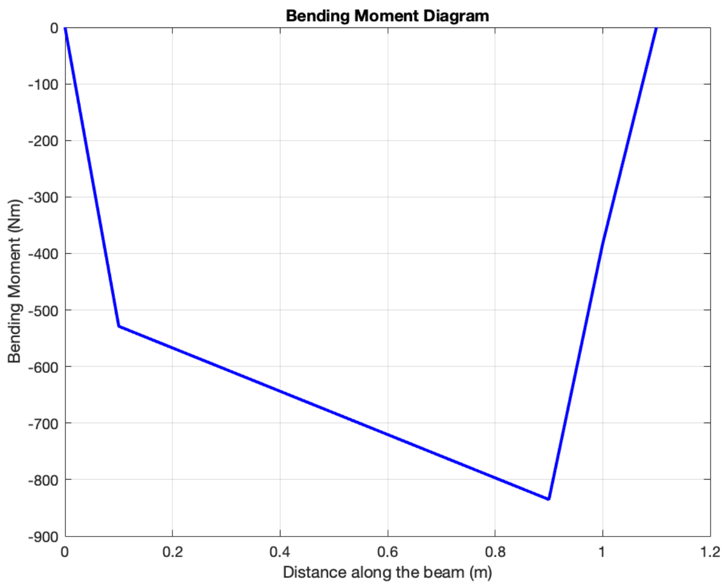

Figure 11 - Design 3 BM Diagram

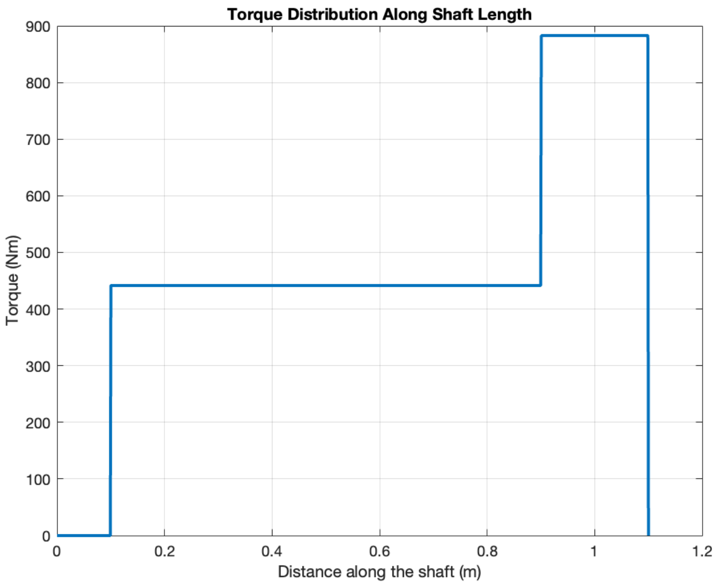

Figure 12 - Design 3 Torque Diagram

2.4.2 Power Transmission

To satisfy the power requirements of a forklift, the design embodied a chain drive chain transmission where the chain selected was a 16B-1, the driving sprocket was a RN16B1Z23B, and the driven sprocket was a RN16B1Z57B.

2.4.3 Material Selection

7 different materials were weighted and ranked based on their stiffness, torsional stiffness and torsional strength relative to their density. From best to worst, the materials rank:

1. CFRP
2. Diamond
3. Carbon Steel AISI 1080
4. Tungsten Carbide-Cobalt 84.02% WC
5. Stainless Steel AM 355
6. 4130 Steel (Low Alloy Steel)
7. Ni-Ti45 (Nitinol)

2.4.4 Manufacturing

Although the merit indices depict *CFRP* and *Diamond* are the most suitable materials, considering financial and manufacturing properties, it was concluded that 4130 Steel had the best ratio between design metrics and performance.

The 30 kW lathe is used for the turning operations involved to manufacture the shaft.

2.4.5 Bearings

Due to the nature of the loading conditions of the shaft, the distributed load across both bearings differ from 5288 N to 692 N. Therefore, through calculations as seen in *Section 3.6*, the bearing choices turned out to be the SKF 6215 and 61818 DGBBs.

2.4.6 Keys, Keyways and Key Seats

The first fork and motor sprocket require a keyway of dimensions 20 mm x 12 mm (b x h), while the second fork sprocket requires a keyway of dimensions 25 mm x 14 mm (b x h). The tolerances of each dimension can be seen in *Table 6*. The lengths of the keys are calculated using the equations referenced in *Equation 2*. The first fork, motor and second fork sprockets have key lengths of 25 mm, 35 mm, and 10 mm respectively.

2.4.7 Circlips

In total, 3 circlips were used for locating the sprockets. Two of these circlips were the SKU DIN 471 D1400 A75 and the other was the SKU DIN 471 D1400 A90, selected from *Figure 26*.

2.5 Design option 4

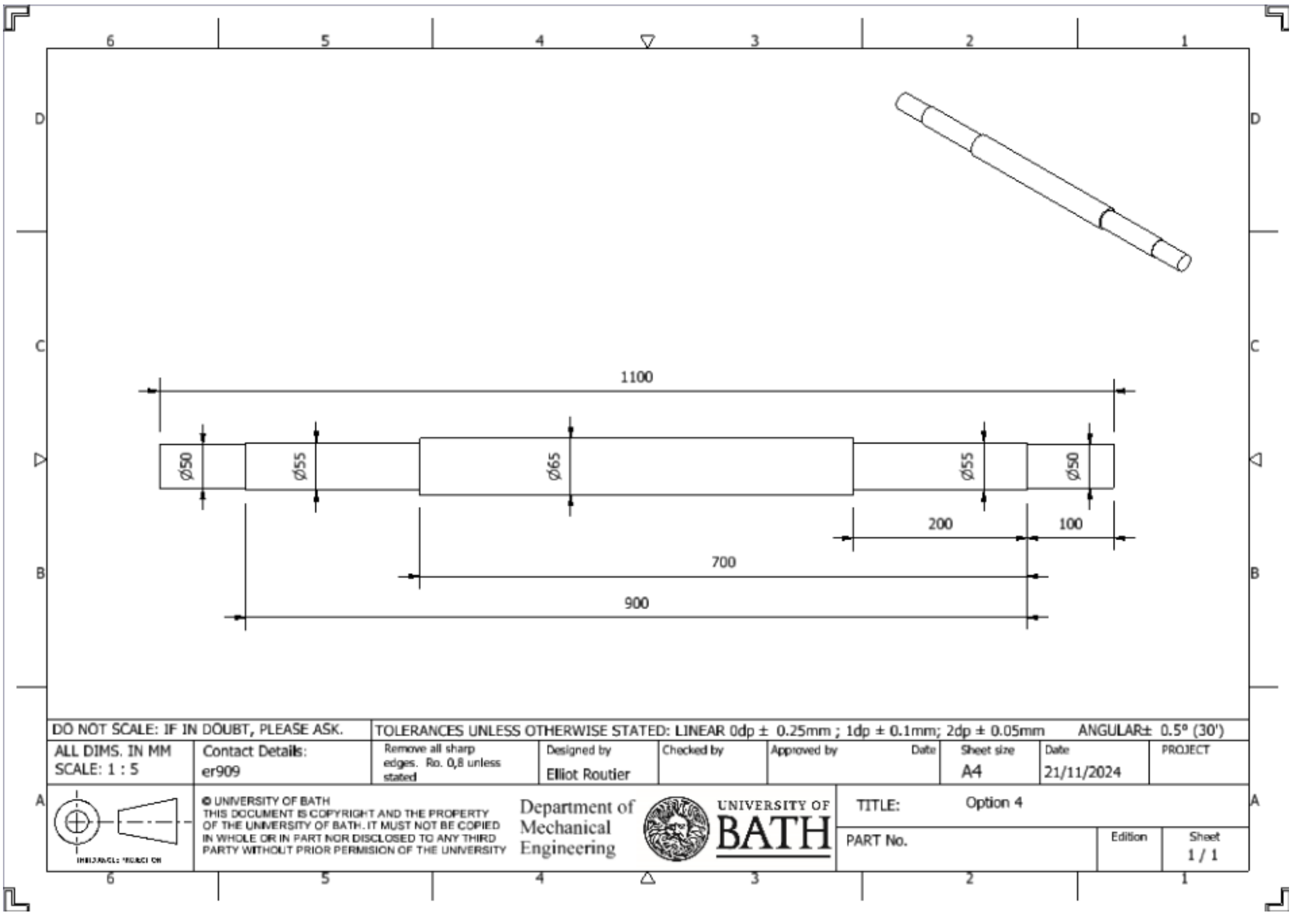

Figure 13 – Basic drawing showing principal dimensions of option 4

2.5.1 Failure calculations

Tabulated in *Appendix 4*, a total of 3 iterations were explored that reduced the percentage failure and passed the von mises criterion.

The final iteration was a stepped shaft ranging from 50 to 65 mm in diameter and stainless-steel AM 355 was used as the material with a design factor of 3. The graphs blow show the bending moments and torque on the shaft:

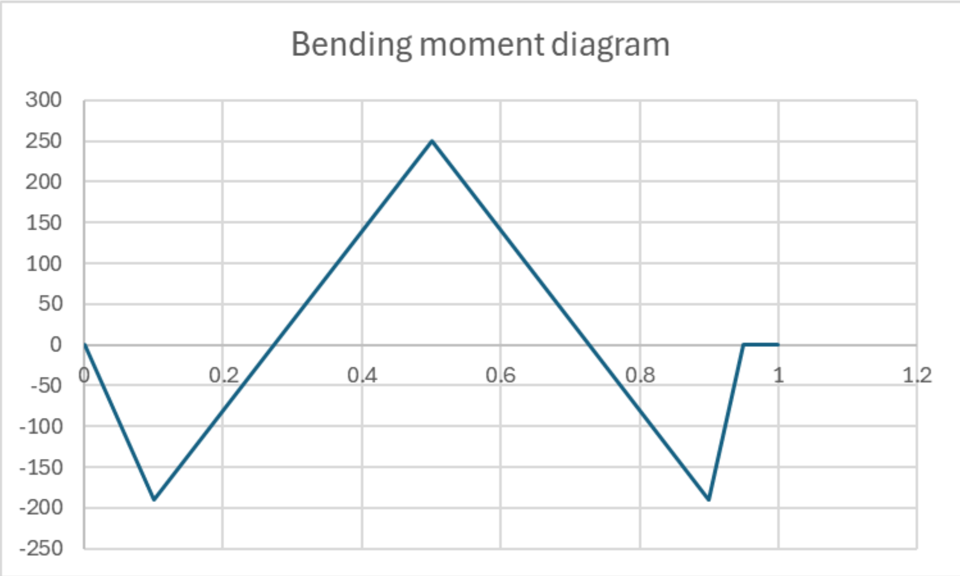

Figure 14- Design 4 Bending Moment Diagram

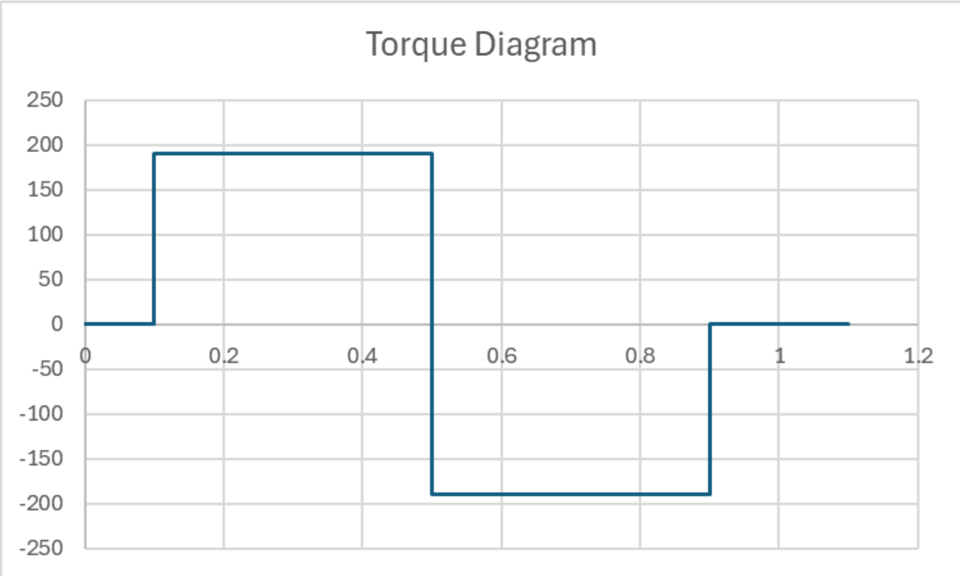

Figure 15 - Design 4 Torque Diagram

2.5.2 Power Transmission

To satisfy the power requirements, the chain selected was a 16B-3, with the corresponding driving sprocket being a 027E0319, and the driven sprocket, 027E0395. The Fenner Roller Chain Selection catalogue was used to determine this.

2.5.3 Material Selection

After using the merit index calculations and Ashby charts, 7 different materials were shortlisted and ranked them based on their stiffness, torsional stiffness and torsional strength relative to their density. This ranking did not cover the manufacturing costs, so the material properties and cost were both factored into when choosing the final material being stainless-steel AM 355.

2.5.4 Manufacturing

The specific energy of stainless-steel AM 355 was relatively low while also maximising material properties in terms of stiffness, torsional stiffness and torsional strength. From *Appendix 4*, the cost of manufacturing to produce option 3's shaft amounts to £6.58. The lathe required to make this shaft is the 10 kW lathe.

2.5.5 Bearings

The load on both bearings was around 760N so the static load rating was 4.3KN and a basic bearing rating of 28 million revolutions, the bearing selected was the 16010 single row deep groove ball bearing.

2.5.6 Keys, keyways and key seats

To transmit torque, the sprockets must be restrained to the shaft using keys. The first and second fork require a keyway of dimensions 20 mm x 12 mm (b x h) with a key length of 25mm, while the motor sprocket requires a keyway of dimensions 25 mm x 14 mm (b x h) and length 25mm as well.

2.5.7 Circlips

In total, 4 circlips were used for the sprockets. Two of these circlips were the DIN 471 DI 400 AA 65 for the driven sprocket and the other two circlips were the DIN 471 DI400 AA 55, selected from the Cirteq circlip catalogue.

3 Final Design

3.1 Design Metrics

The following design metrics were evaluated between the 4 individual designs:

- Manufacturing Cost and Time
- Shaft volume
- Shaft weight
- Cost of material

Design option	Design metrics				
	manufacturing cost (£)	manufacturing time (s)	Volume (m^3)	Shaft weight (N)	cost of material (£)
Option 1	2.27	120	3.72E-03	104	55.8
Option 2	13	645	3.52E-03	847.1	54.3
Option 3	5.8	227	6.86E-03	528.3	61
Option 4	6.58	298	2.86E-03	220	44.6

Table 1 - Details the design metrics for each option.

Comparing the design metrics between options 1, 2, 3 and 4, option 1 seems to be the best because it has:

- The lowest manufacturing cost
- The lowest manufacturing time
- The second smallest volume
- The smallest weight
- The third lowest cost of material

For these reasons, option 1 was selected as the final design.

3.2 Final Design Changes

Compared to option 1, the final design changed:

- The design factor was updated to 5.46 from option 3
- Motor angle inclined to 30 degrees to the horizontal
- Some shaft dimensions to meet design requirements
- Stress concentration factors
- Transmission – Teeth on driving sprocket changed to option 2 as it was more compact

3.3 Calculations

The shaft was modelled as a beam with three forces acting on it, one from each sprocket with supports from the bearings on each end. The aim of the calculations was to deduce the maximum load at each critical point along the shaft and compare it to the yield strength of the chosen material to ensure it doesn't fail.

The forces along the shaft were distributed as follows:

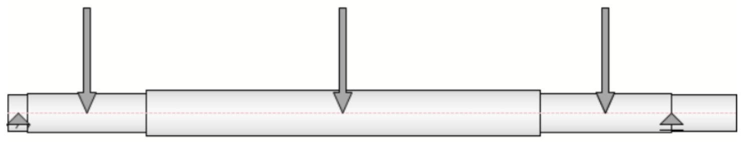

Figure 16 - Free body diagram of the shaft. Note that although the outermost arrows are modelled as vertically downwards, the component of force due to the sprockets in these positions are vertically upwards. The bearings are located on the ends of the shaft.

The bending moment and torque distribution along the shaft is as follows:

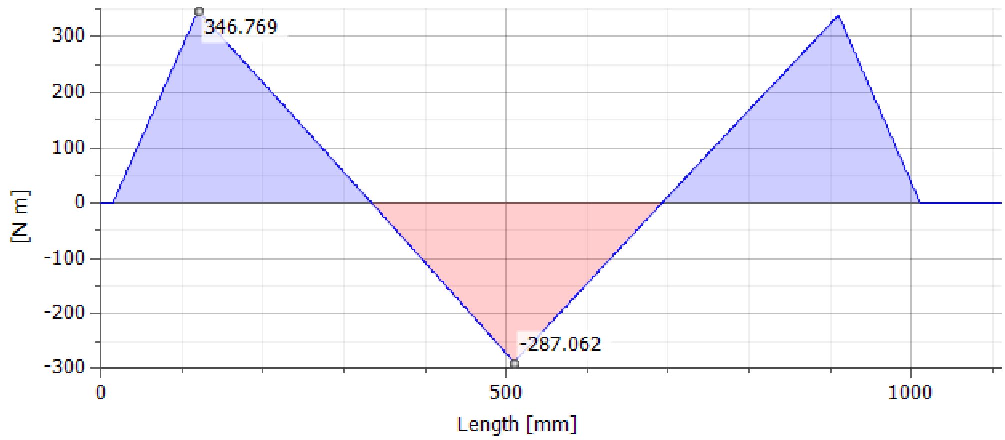

Figure 17 - The vertical bending moment along the length of the shaft.

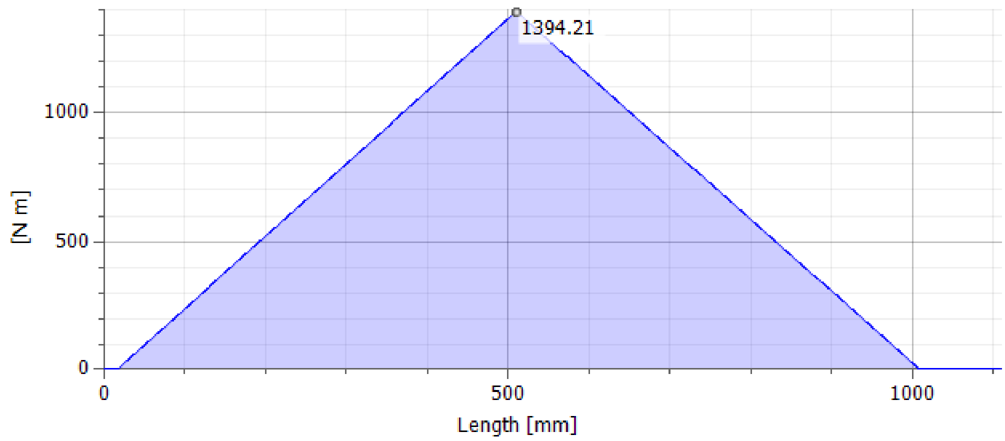

Figure 18 - the horizontal bending moment along the length of the shaft

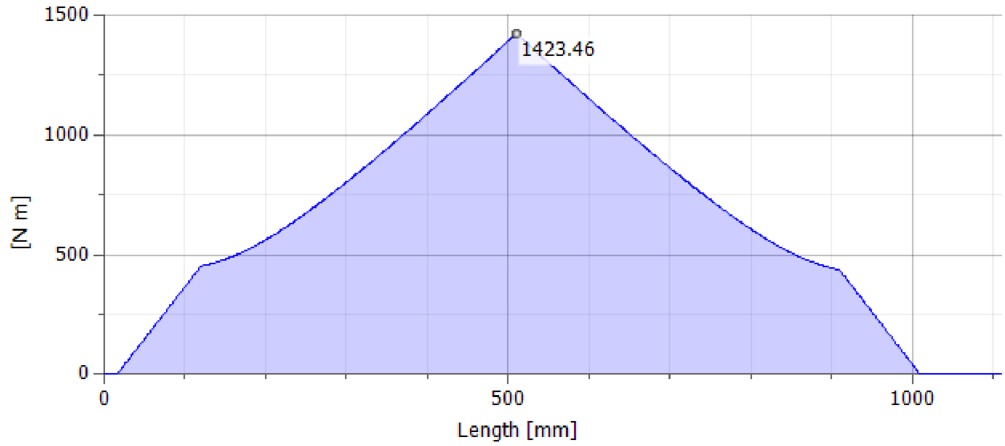

Figure 19 - The combined bending moment diagram along the length of the shaft accounting for the vertical and horizontal bending moments.

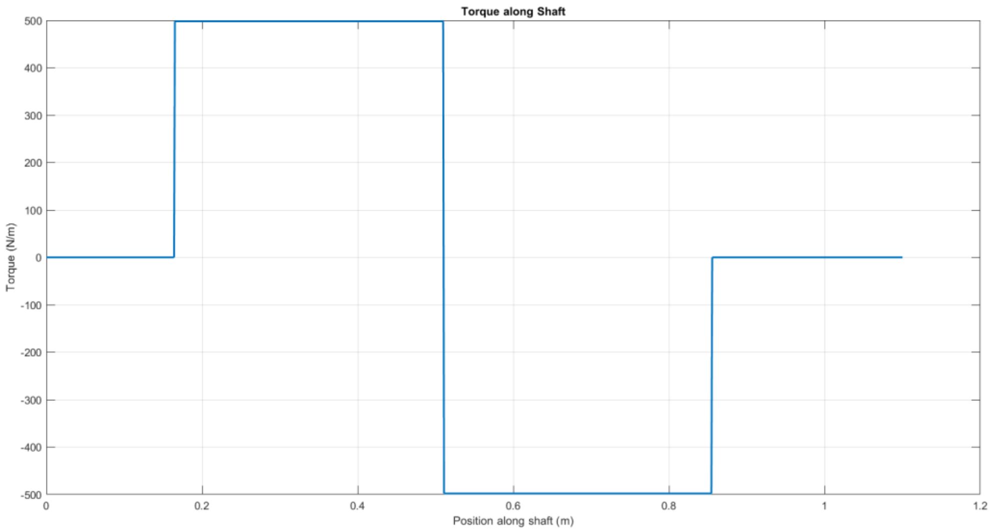

Figure 20 - Torque distribution along the length of the shaft.

The failure calculations for the shaft were recycled from option 1:

			Nodes										
Parameter	**Symbol**	**Unit**		**Sprocket 1**			**Sprocket 2**			**Sprocket 3**			
			Shoulder	Circlip Groove	Keyseat	Shoulder	Circlip Groove	Keyseat	Circlip Grove	Shoulder	Keyseat	Circlip Groove	Shoulder
Diameter	d	m	0.055	0.06	0.06	0.06	0.07	0.07	0.07	0.06	0.06	0.06	0.06
Cross Sectional Area	A	m^2	0.002375829	0.002827433	0.002827433	0.002827433	0.003848451	0.003848451	0.003848451	0.002827433	0.002827433	0.002827433	0.002827433
Bending moment Vertical			0	347	347	347	-287	-287	-287	347	347	347	0
Bending Moment Horizontal			0	310	310	310	1394	1394	1394	310	310	310	0
Bending Moment Combined	M	Nm	0	465.3052761	465.3052761	465.3052761	1423.237507	1423.237507	1423.237507	465.3052761	465.3052761	465.3052761	0
Torque	T	Nm	0	500	500	500	-500	-500	-500	0	0	0	0
Bending SCF	Km	-	1.59	2	2.1	1.71	1.8	2.1	1.8	1.71	2.1	2	1.59
Torsion SCF	Ks	-	1.31	1.8	3	1.39	1.6	3	1.6	1.39	3	1.8	1.31
Distance from Neutral Axis	y	m	0.0275	0.03	0.03	0.03	0.035	0.035	0.035	0.03	0.03	0.03	0.03
Second Moment of Area	I	m^4	4.4918E-07	6.36173E-07	6.36173E-07	6.36173E-07	1.17859E-06	1.17859E-06	1.17859E-06	6.36173E-07	6.36173E-07	6.36173E-07	6.36173E-07
Nominal Normal Stress	σ_Mn	Pa	0	21942410.29	21942410.29	21942410.29	42265242.56	42265242.56	42265242.56	21942410.29	21942410.29	21942410.29	0
Actual Normal Stress	σ_M	Pa	0	43884820.59	46079061.62	37521521.6	76077436.61	88757009.38	76077436.61	37521521.6	46079061.62	43884820.59	0
Polar Moment of Area	J	m^4	8.98361E-07	1.27235E-06	1.27235E-06	1.27235E-06	2.35718E-06	2.35718E-06	2.35718E-06	1.27235E-06	1.27235E-06	1.27235E-06	1.27235E-06
Nominal Torsion Stress	τ_n	Pa	0	11789255.04	11789255.04	11789255.04	-7424137.287	-7424137.287	-7424137.287	0	0	0	0
Actual Torsion Stress	τ	Pa	0	21220659.08	35367765.13	16387064.51	-11878619.66	-22272411.86	-11878619.66	0	0	0	0
Combined Stress	Sa	Pa	0	57243572.51	76654525.96	47047552.89	78810412.87	96778033.17	78810412.87	37521521.6	46079061.62	43884820.59	0
Combined Stress * Ny	Sa * Ny	Pa	0	312549905.9	418533711.8	256879638.8	430304854.3	528408061.1	430304854.3	204867508	251591676.4	239611120.4	0
Validity	V	%	0	44.64998656	59.79053025	36.69709126	61.47212204	75.48686587	61.47212204	29.26678685	35.94166806	34.23016006	0

Table 2 - Tabulates all the calculations based on the bending moment and torque diagrams that were generated in Figures 17 - 20

The design factor, N_y is calculated using the equation:

$$N_y = b \cdot c \cdot d$$

Equation 1 - Finding the design factor where b = 1.5 and c = 2.

d is determined from the equation d = X Y. X and Y can be calculated from these tables:

A =	B = C =	VG	G	F	P
VG	VG	1.1	1.3	1.5	1.7
VG	G	1.2	1.45	1.7	1.95
VG	F	1.3	1.6	1.9	2.2
VG	P	1.4	1.75	2.1	2.45
G	VG	1.4	1.55	1.8	2.05
G	G	1.45	1.75	2.05	2.35
G	F	1.6	1.95	2.3	2.65
G	P	1.75	2.15	2.55	2.95
F	VG	1.5	1.8	2.1	2.4
F	G	1.7	2.05	2.4	2.75
F	F	1.9	2.3	2.7	3.1
F	P	2.1	2.55	3.00	3.45
P	VG	1.7	2.15	2.4	2.75
P	G	1.95	2.35	2.75	3.15
P	F	2.2	2.65	3.1	3.55
P	P	2.45	2.95	3.45	3.95

Table 3 - Table to determine coefficient X based on the quality of the component in three areas: materials, workshop, inspection and manufacture, loading and control over it, and quality of assessment of strength, analysis methods and accuracy.

D = E =	Not Serious	Serious	Very Serious
Not Serious	1	1.2	1.4
Serious	1.1	1.3	1.5
Very Serious	1.2	1.4	1.6

Table 4 - To calculate the value of Y, one must assess the potential impact of the failing with respect to two areas: D; Seriousness of danger to personnel and E; Seriousness of economic consequences.

3.4 Power Transmission

The chain drive transmission was selected from Option 2 where the chain chosen was a 16B-1, the driving sprocket was a RN16B1Z21B, and the driven sprocket was a RN16B1Z38B. The following table shows the calculations which derived to the chosen transmission:

Power Transmission Calculations			
Parameters	**Symbol**	**Units**	**Value**
Fork Velocity	v1	m/s	0.1
Fork Sprocket Radius	r1	m	0.09
Driven Sprocket Radius	r2	m	0.154
Shaft Angular Velocity	ω1	rad/s	1.111111
Driven Sprocket Velocity	v2	m/s	0.171111
Transmission Power	Pt	W	982.3078
Force Motor	Fm	N	5740.76
Application Factor	f1	-	1.5
Tooth Factor	f2	-	0.76
Selection Power	Ps	W	1119.831
Driving Teeth	Z1	-	21
Driven Teeth	Z2	-	38
Centre Distance	C1	m	1.016
Chain Pitch	P	m	0.0254
Chain Length	L	m	2.785948
Drive Ratio	i	-	1.809524
Motor Angular Velocity	ω2	rad/s	19.19964

Table 5 - Presents the calculations of the power transmission to arrive to the chosen chain and sprockets used for the power transmission from the motor to the shaft.

The data from *Table 5* was then used with the following graphs from the Reynolds catalogue to determine the chains and sprockets:

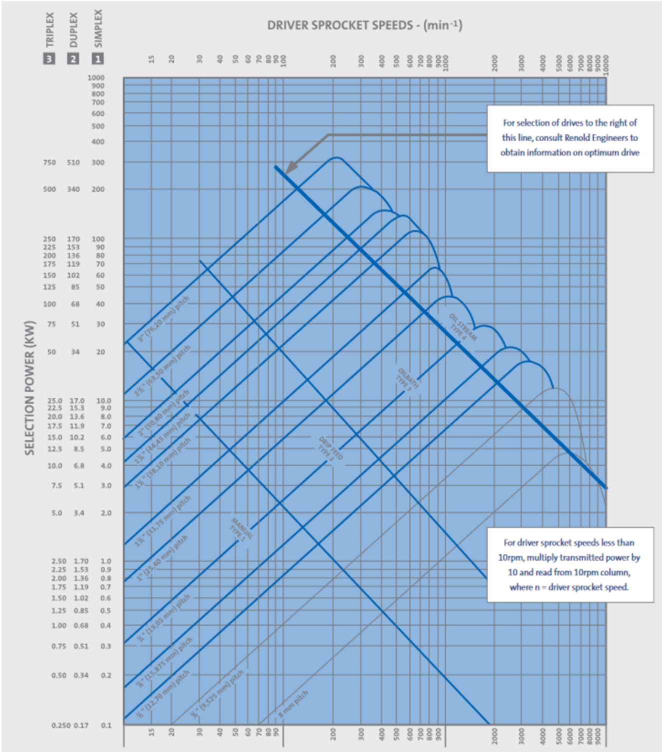

Figure 21 - Shows the pitch of the chain for a simplex, duplex or triplex chain depending on the selection power and the sprocket angular speed.

Number of teeth	PCD Factor	Number of teeth	PCD Factor	Number of teeth	PCD Factor
9	2.924	57	18.153	105	33.428
10	3.236	58	18.471	106	33.746
11	3.549	59	18.789	107	34.064
12	3.864	60	19.107	108	34.382
13	4.179	61	19.426	109	34.701
14	4.494	62	19.744	110	35.019
15	4.810	63	20.062	111	35.337
16	5.126	64	20.380	112	35.655
17	5.442	65	20.698	113	35.974
18	5.759	66	21.016	114	36.292
19	6.076	67	21.335	115	36.610
20	6.392	68	21.653	116	36.928
21	6.709	69	21.971	117	37.247
22	7.027	70	22.289	118	37.565
23	7.344	71	22.607	119	37.883
24	7.661	72	22.926	120	38.202
25	7.979	73	23.244	121	38.520
26	8.296	74	23.562	122	38.838
27	8.614	75	23.880	123	39.156
28	8.931	76	24.198	124	39.475
29	9.249	77	24.517	125	39.793
30	9.567	78	24.835	126	40.111
31	9.885	79	25.153	127	40.429
32	10.202	80	25.471	128	40.748
33	10.520	81	25.790	129	41.066
34	10.838	82	26.108	130	41.384
35	11.156	83	26.426	131	41.703
36	11.474	84	26.744	132	42.021
37	11.792	85	27.063	133	42.339
38	12.110	86	27.381	134	42.657
39	12.428	87	27.699	135	42.976
40	12.746	88	28.017	136	43.294
41	13.063	89	28.335	137	43.612
42	13.382	90	28.654	138	43.931
43	13.700	91	28.972	139	44.249
44	14.018	92	29.290	140	44.567
45	14.336	93	29.608	141	44.885
46	14.654	94	29.927	142	45.204
47	14.972	95	30.245	143	45.522
48	15.290	96	30.563	144	45.840
49	15.608	97	30.881	145	46.159
50	15.926	98	31.200	146	46.477
51	16.244	99	31.518	147	46.795
52	16.562	100	31.836	148	47.113
53	16.880	101	32.154	149	47.432
54	17.198	102	32.473	150	47.750
55	17.517	103	32.791		
56	17.835	104	33.109		

Figure 22 - Used to determine the number of teeth on the sprocket based on the PCD factor.

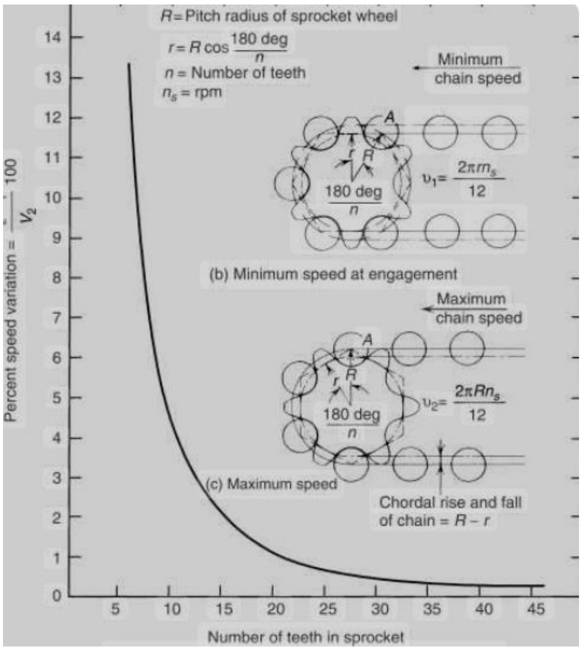

Figure 23 - Visual representation of the polygonal effect. It demonstrates why there should never be less than 19 teeth on a sprocket as the percentage speed fluctuation increase rapidly beyond this number of teeth

3.5 Keys, keyways and key seats

Dimensions and tolerances for keys, key seats and keyways can be determined from the following table and equations, depending on the shaft diameter and loading conditions respectively:

Key lengths can be determined via the following Equations:

$$l_1 = \frac{\sqrt{3}FN_y}{bS_y}, \quad l_2 = \frac{2FN_y}{hS_y}$$

Equation 2 - Determines the minimum length of the key such that they do not break.

Table 3 — Dimensions and tolerances of keyways for rectangular parallel keys

All dimensions in millimetres

1	2	3	4	5	6	7	8	9	10	11	12	13	14	15
Shaft		Key (see Note)	Keyway											
nominal diameter (see Note) d		section $b \times h$ width × thickness	width b						depth				radius r	
				tolerance for class of fit					shaft t_1		hub t_2			
				free		normal		close and interference						
over	incl.		nom.	shaft (H9)	hub (D10)	shaft (N9)	hub (J$_s$9)[a]	shaft and hub (P9)	nom.	tol.	nom.	tol.	max.	min.
22	30	8 × 7	8	+ 0.036	+ 0.098	0	+ 0.018	− 0.015	4		3.3		0.25	0.16
30	38	10 × 8	10	0	+ 0.040	− 0.036	− 0.018	− 0.051	5		3.3		0.40	0.25
38	44	12 × 8	12						5		3.3		0.40	0.25
44	50	14 × 9	14	+ 0.043	+ 0.120	0	+ 0.021	− 0.018	5.5		3.8		0.40	0.25
50	58	16 × 10	16	0	+ 0.050	− 0.043	− 0.021	− 0.061	6	+ 0.2	4.3	+ 0.2	0.40	0.25
58	65	18 × 11	18						7	0	4.4	0	0.40	0.25
65	75	20 × 12	20						7.5		4.9		0.60	0.40
75	85	22 × 14	22	+ 0.052	+ 0.149	0	+ 0.026	− 0.022	9		5.4		0.60	0.40
85	95	25 × 14	25	0	+ 0.065	− 0.052	− 0.026	− 0.074	9		5.4		0.60	0.40
95	110	28 × 16	28						10		6.4		0.60	0.40
110	130	32 × 18	32						11		7.4		0.60	0.40
130	150	36 × 20	36	+ 0.062	+ 0.180	0	+ 0.031	− 0.026	12		8.4		1.00	0.70
150	170	40 × 22	40	0	+ 0.080	− 0.062	− 0.031	− 0.088	13		9.4		1.00	0.70
170	200	45 × 25	45						15		10.4		1.00	0.70
200	230	50 × 28	50						17		11.4		1.00	0.70
230	260	56 × 32	56						20	+ 0.3	12.4	+ 0.3	1.60	1.20
260	290	63 × 32	63	+ 0.074	+ 0.220	0	+ 0.037	− 0.032	20	0	12.4	0	1.60	1.20
290	330	70 × 36	70	0	+ 0.100	− 0.074	− 0.037	− 0.106	22		14.4		1.60	1.20
330	380	80 × 40	80						25		15.4		2.50	2.00
380	440	90 × 45	90	+ 0.087	+ 0.260	0	+ 0.043	− 0.037	28		17.4		2.50	2.00
440	500	100 × 50	100	0	+ 0.120	− 0.087	− 0.043	− 0.124	31		19.5		2.50	2.00

NOTE The relations between shaft diameter and key section given above are for general applications. The use of smaller key sections is permitted if suitable for the torque transmitted. In cases such as stepped shafts when larger diameters are required, for example to resist bending, and when fans, gears and impellers are fitted with a smaller key than normal, an unequal disposition of key in shaft with relation to the hub results. Therefore, dimensions $d - t_1$ and $d + t_2$ should be recalculated to maintain the $h/2$ relationship.
The use of larger key sections which are special to any particular application is outside the scope of this standard.

[a] The limits for tolerance J$_s$9 are quoted from BS 4500, "ISO limits and fits", to three significant figures.

Table 6 - Tabulates key, keyway and key seat dimensions along with their respective tolerances.

Three keys are used on the shaft. Two of which sit on the 60mm diameter of the shaft and one on the 70 mm diameter section of the shaft:

Loads

Power	P	0.555 kW
Speed	n	10.600 rpm
Torque	T	500.000 N m

Dimensions

Shaft Diameter	d	60.00000 mm
Hollow Shaft Inner Diameter	d_h	0.000 mm

Key

Key Width	b	18.000 mm
Key Height	h	11.000 mm
Key Length	l	63.000 mm
Functional Length	l_f	27.595 mm
Key Chamfer	s	0.600 mm
Key Radius	R	0.160 mm

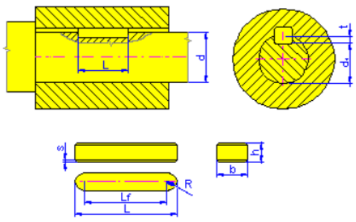

Joint Properties

Number of Keys	N	1.000 ul
Application Factor	K_a	1.000 ul
Fatigue-Life Factor	K_f	1.000 ul
Wear-Life Factor	K_w	1.000 ul
Load Distribution Factor	K_m	1.000 ul
Desired Safety	S_v	2.000 ul

Figure 24: Shows the principal dimensions of the keys sitting on the 60 mm diameter section of the shaft. These include the key length, key width, key height and functional length of the key. Tolerances for the keyway and key seat can be selected from Table 6.

Loads

Power	P	0.838 kW
Speed	n	16.000 rpm
Torque	T	500.000 N m

Dimensions

Shaft Diameter	d	70.00000 mm
Hollow Shaft Inner Diameter	d_h	0.000 mm

Key

Key Width	b	20.000 mm
Key Height	h	12.000 mm
Key Length	l	56.000 mm
Functional Length	l_f	6.085 mm
Key Chamfer	s	0.800 mm
Key Radius	R	0.160 mm

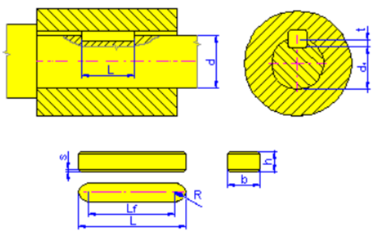

Joint Properties

Number of Keys	N	1.000 ul
Application Factor	K_a	1.000 ul
Fatigue-Life Factor	K_f	1.000 ul
Wear-Life Factor	K_w	1.000 ul
Load Distribution Factor	K_m	1.000 ul
Desired Safety	S_v	1.000 ul

Figure 25: Shows the principal dimensions of the keys sitting on the 70 mm diameter section of the shaft. These include the key length, key width, key height and functional length of the key. Tolerances for the keyway and key seat can be selected from Table 6.

3.6 Bearing Selection

Roller bearings could not be used due to their inability to withstand any axial load. Deep groove ball bearings were used as unlike roller bearings, they can absorb both vertical and axial loads, providing greater safety in case of a malfunction.

$$L_{10} = \left(\frac{C}{P}\right)^{p}$$

Equation 3 - Basic Bearing Life Rating (90% Reliability)

Where:

- $P = Equivalent\ Dynamic\ Bearing\ Load\ /\ Fatigue\ Load\ Rating\ (kN)$
- $L_{10} = Basic\ Rating\ Life\ ,at\ 90\%\ Reliability$ (million revs)
- $C = Basic\ Dynamic\ Load\ Rating\ of\ the\ Bearing\ (kN)$
- $p = 3\ for\ Ball\ Bearings$

Selecting Bearings:

- The Bearing should be able to withstand constant operation for 12 hours a day, every day for 10 years:

$$L_{10} = 10.61\, rpm \times 60 \times 12 \times 365.25 \times 10 = 27.9\, million\, revs$$

- Through resolving the dynamic loading conditions of the shaft, on Bearing A, the resultant force calculated was:

$$C = 4.633\, kN$$

- Using the formula above, we rearrange for P (Fatigue Load P_0), to see the required designation for a specific bearing with a bore of 55mm in diameter:

$$P_0 = \frac{C}{L_{10}^{1/3}} = \frac{4.633 \times 10^3}{(27.9 \times 10^6)^{1/3}} = 1.582\, kN$$

- This process was then repeated for the 2nd bearing, giving the following values seen in *Table 7:*

Bearing 6311	Fatigue Load Limit 1.9 kN (> 1.582 AND >1.367)
Seal	Contact Seal RSH
Housing SNL 213	Sealed and End Capped
Locating Rings FRB 11/120	2 Locating rings adjacent to bearing in the bearing seat

Table 7 - Lubricated bearing housings: prevent contamination from outside, as well as to axially restrain the bearings to the shaft in tandem with the locating rings. Bearing: The bearing chosen was SKF 6311. The bearings come pre-shielded with 2 RSH Contact seals further providing an effective sealing and protection.

Bearing 1 on a Shaft Diameter of 55 mm			
P_0	Static Loading	kN	4.905
s_0	Safety Factor		1
C_0	Static Load Rating		4.905
ω_s	Angular Speed of Shaft	rad/s	1.1111111
		rpm	10.61032943
L_10	Basic Life Rating	revs	27903044.34
C_1	Dynamic Load Rating	kN	4.633
P_1	Equiv. Dynamic Load	kN	1.582089084

Table 8 - Calculations for Bearing A

Bearing 2 on a Shaft Diameter of 55 mm			
P_0	Static Loading	kN	4.905
s_0	Safety Factor		1
C_0	Static Load Rating		4.905
ω_s	Angular Speed of Shaft	rad/s	1.1111111
		rpm	10.61032943
L_10	Basic Life Rating	revs	27903044.34
C_1	Dynamic Load Rating	kN	4.004
P_1	Equiv. Dynamic Load	kN	1.367296502

Table 9 – Calculations for Bearing B

3.7 Circlips

For the final design iteration, 4 circlips were used for locating the sprockets. Two of these circlips were the DIN 471 DI 400 AA 70 and the other two circlips were the DIN 471 DI400 AA 60. Selected from the Cirteq circlip catalogue:

Circlips pour arbres **Sicherungsringe für Wellen** Anillos para ejes **RINGS FOR SHAFTS**

d_1	DIN 471 D1400 A	s	Δ	d_3	Δ	a max.	b ≈	d_5 min.	C_1	C_2	(kg/1000)
38	A38	1.75		35.2		5.8	4.2	2.5	50.2	47.6	5.620
39	A39	1.75		36.0	+0.25/−0.50	5.9	4.3	2.5	51.4	48.5	5.850
40	A40	1.75		36.5		6.0	4.4	2.5	52.6	49.5	6.030
41	A41	1.75		37.5		6.2	4.5	2.5	54.0	51.5	6.215
42	A42	1.75		38.5		6.5	4.5	2.5	55.7	52.5	6.500
44	A44	1.75	−0.06	40.5		6.6	4.6	2.5	57.9	55.4	7.000
45	A45	1.75		41.5		6.7	4.7	2.5	59.1	55.9	7.500
46	A46	1.75		42.5	+0.39	6.7	4.8	2.5	60.1	56.9	7.600
47	A47	1.75		43.5	−0.90	6.8	4.9	2.5	61.3	58.1	7.500
48	A48	1.75		44.5		6.9	5.0	2.5	62.5	59.3	7.900
50	A50	2.00		45.8		6.9	5.1	2.5	64.5	60.8	10.20
52	A52	2.00		47.8		7.0	5.2	2.5	66.7	63.0	11.10
54	A54	2.00		49.8		7.1	5.3	2.5	69.0	65.2	11.30
55	A55	2.00		50.8		7.2	5.4	2.5	70.2	66.4	11.40
56	A56	2.00		51.8		7.3	5.5	2.5	71.6	67.6	11.80
57	A57	2.00		52.8		7.3	5.5	2.5	72.3	69.3	12.20
58	A58	2.00		53.8		7.3	5.6	2.5	73.6	69.6	12.60
60	A60	2.00		55.8		7.4	5.8	2.5	75.6	71.8	12.90
62	A62	2.00		57.8		7.5	6.0	2.5	77.8	74.0	14.30
63	A63	2.00	−0.07	58.8		7.6	6.2	2.5	79.0	75.2	15.90
65	A65	2.50		60.8		7.8	6.3	3.0	81.4	77.6	18.20
67	A67	2.50		62.5	+0.46	7.9	6.4	3.0	83.6	79.8	20.30
68	A68	2.50		63.5	−1.10	8.0	6.5	3.0	84.4	81.0	21.80
70	A70	2.50		65.5		8.1	6.6	3.0	87.0	83.2	22.00
72	A72	2.50		67.5		8.2	6.8	3.0	89.2	85.4	22.50
75	A75	2.50		70.5		8.4	7.0	3.0	92.7	88.8	24.60
77	A77	2.50		72.5		8.5	7.2	3.0	94.9	91.0	25.70
78	A78	2.50		73.5		8.6	7.3	3.0	96.1	92.2	26.20
80	A80	2.50		74.5		8.6	7.4	3.0	98.1	93.7	27.30
82	A82	2.50		76.5		8.7	7.6	3.0	100.3	95.9	31.20
85	A85	3.00		79.5		8.7	7.8	3.5	103.3	98.9	36.40
87	A87	3.00		81.5		8.8	7.9	3.5	105.5	100.9	39.80
88	A88	3.00	−0.08	82.5		8.8	8.0	3.5	106.5	102.0	41.20
90	A90	3.00		84.5	+0.54	8.8	8.2	3.5	108.5	104.0	44.50
92	A92	3.00		86.5	−1.30	9.0	8.4	3.5	110.9	107.4	46.00

d_1	d_2	Δ	m min.	t	n	FN (kN)	FR (kN)	g	FRg (kN)	AN (mm²)	B	$n_{det.}$ x1000 (rpm)
38	36.0		1.85	1.00	3.0	19.3	49.5	2.0	9.10	116	95.0	14
39	37.0		1.85	1.00	3.0	19.9	49.8	2.0	9.25	119	95.2	15
40	37.5		1.85	1.25	3.8	25.3	51.0	2.0	9.50	152	97.0	14
41	38.5		1.85	1.25	3.8	26.0	50.1	2.0	9.40	156	94.5	14
42	39.5		1.85	1.25	3.8	26.7	50.0	2.0	9.45	160	93.7	13
44	41.5	−0.25	1.85	1.25	3.8	28.0	48.5	2.0	9.20	168	90.7	12
45	42.5		1.85	1.25	3.8	28.6	49.0	2.0	9.35	172	91.0	11
46	43.5		1.85	1.25	3.8	29.4	48.9	2.0	9.40	177	90.2	11
47	44.5		1.85	1.25	3.8	30.0	49.5	2.0	9.55	180	90.7	11
48	45.5		1.85	1.25	3.8	30.7	49.4	2.0	9.55	184	90.0	10
50	47.0		2.15	1.50	4.5	38.0	73.3	2.0	14.40	228	133.0	11
52	49.0		2.15	1.50	4.5	39.7	73.1	2.5	11.50	238	133.0	10
54	51.0		2.15	1.50	4.5	41.2	71.2	2.5	11.30	247	129.0	9
55	52.0		2.15	1.50	4.5	42.0	71.4	2.5	11.40	252	130.0	9
56	53.0		2.15	1.50	4.5	42.8	70.8	2.5	11.30	257	129.0	9
57	54.0		2.15	1.50	4.5	43.7	70.9	2.5	11.40	262	128.0	8
58	55.0		2.15	1.50	4.5	44.3	71.1	2.5	11.50	266	129.0	8
60	57.0		2.15	1.50	4.5	46.0	69.2	2.5	11.30	276	126.0	8
62	59.0		2.15	1.50	4.5	47.5	69.3	2.5	11.40	285	126.0	7
63	60.0		2.15	1.50	4.5	48.3	70.2	2.5	11.60	290	126.0	7
65	62.0	−0.30	2.65	1.50	4.5	49.8	135.0	2.5	22.70	299	245.0	7
67	64.0		2.65	1.50	4.5	51.3	136.0	2.5	23.00	308	245.0	7
68	65.0		2.65	1.50	4.5	52.2	135.0	2.5	23.10	313	244.0	7
70	67.0		2.65	1.50	4.5	53.8	134.0	2.5	23.00	323	241.0	7
72	69.0		2.65	1.50	4.5	55.3	131.0	2.5	22.80	332	236.0	6
75	72.0		2.65	1.50	4.5	57.6	130.0	2.5	22.80	346	234.0	6
77	74.0		2.65	1.50	4.5	59.3	131.0	3.0	19.70	356	238.0	6
78	75.0		2.65	1.50	4.5	60.0	131.0	3.0	19.70	360	239.0	5
80	76.5		2.65	1.75	5.3	71.6	128.0	3.0	19.50	430	236.0	6
82	78.5		2.65	1.75	5.3	73.5	128.0	3.0	19.60	441	237.0	6
85	81.5		3.15	1.75	5.3	76.2	215.0	3.0	33.40	457	405.0	6
87	83.5		3.15	1.75	5.3	78.2	222.0	3.0	34.80	469	405.0	5
88	84.5	−0.35	3.15	1.75	5.3	79.0	221.0	3.0	34.80	474	406.0	5
90	86.5		3.15	1.75	5.3	80.0	217.0	3.0	34.40	485	401.0	5
92	88.5		3.15	1.75	5.3	82.0	217.0	3.5	29.60	496	404.0	5

Part Number Référence Teile Nummer Referencia de pieza — **Tolerance** Tolérance Toleranz Tolerancia — **Weight** Masse Gewicht Peso — **Ring** Anneau/Circlips Ring Anillo — **Groove** Gorge Nut Ranura

Figure 26: the Cirteq circlip catalogue table from which the circlips were determined. These also specify the circlip groove dimensions and tolerances.

3.9 Stress Concentration Factors

Stress concentration factors were determined from the R. E. Peterson, “Design Factors for Stress Concentration” Machine Design, vol. 23 catalogue. *Figure 7* tabulates the bending and torsional stress concentration factors of circlip grooves and shoulders.

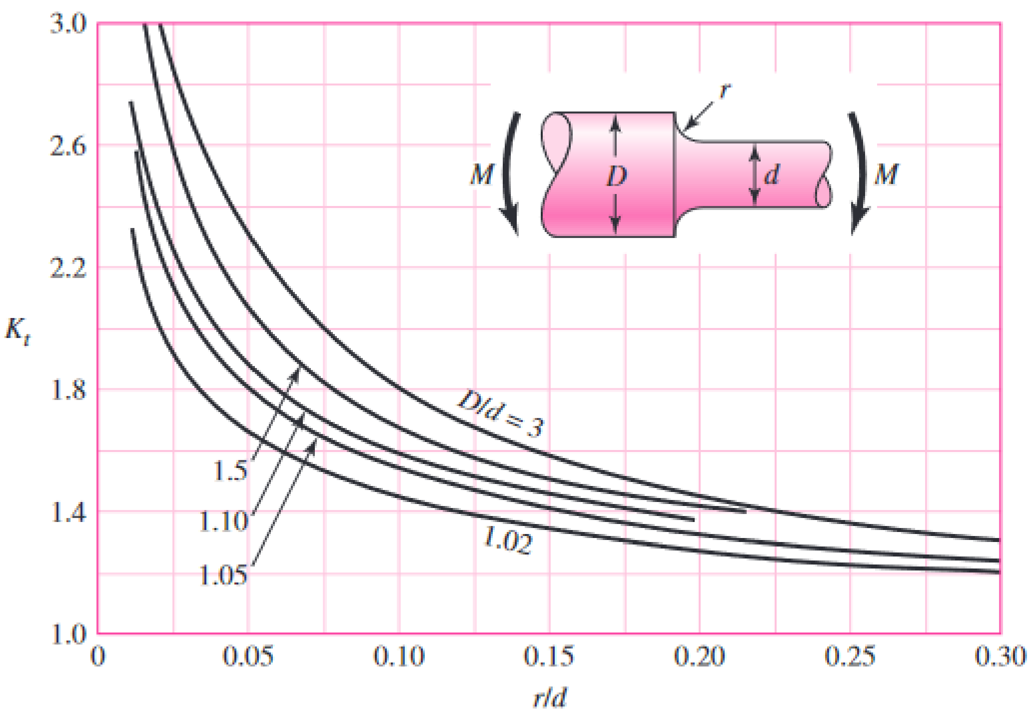

Figure 27: Graph used to determine the bending stress concentration factors on the shoulders of the shaft.

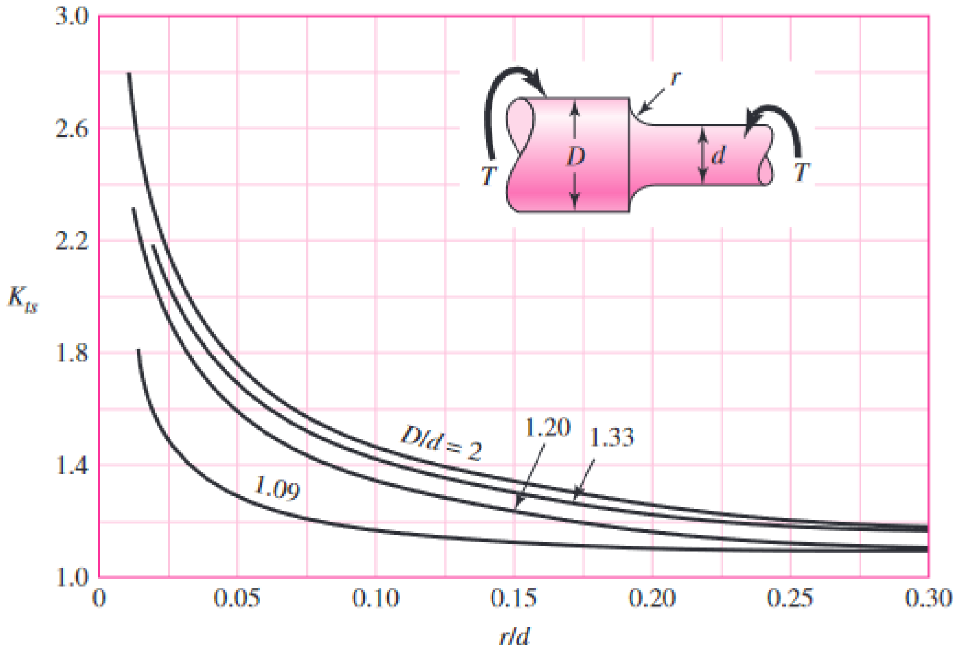

Figure 28: Graph used to determine the torsional stress concentration factors on the shoulders of the shaft.

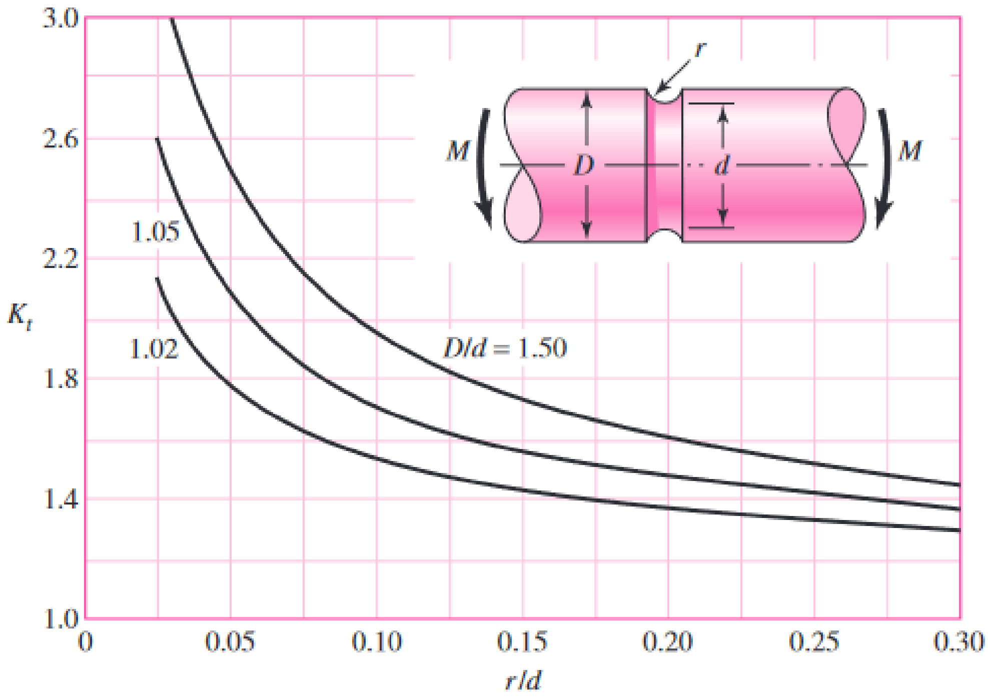

Figure 29: Graph used to determine the bending stress concentration factors for the circlip grooves on the shaft.

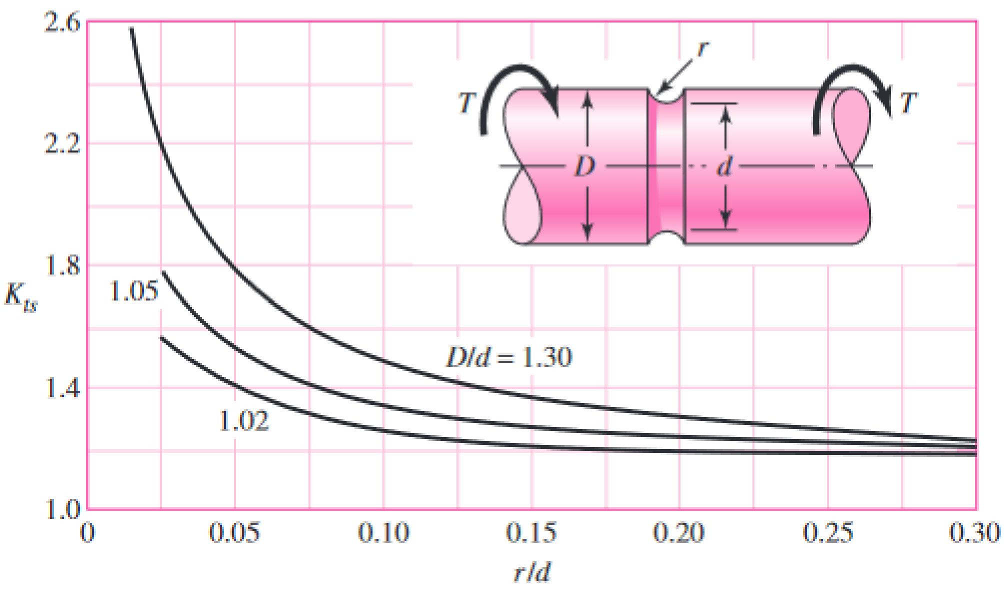

Figure 30: Graph used to determine the torsional stress concentration factors for the circlip grooves on the shaft.

The stress concentration factors for key seats were provided by Rick Lupton:

- 2.1 for the bending stress concentration factors
- 3.0 for the torsional stress concentration factors

3.8 Material Selection

Seven different materials were initially screened and are listed in *Table 10*. These seven materials were selected as candidates in the initial screening as they were positioned above the merit index slope of the Ashby chart as seen in *Figure 34*.

Material	Density (kg/m^3)	Yield Strength (MPa)	Fatigue Strength (MPa)	Young's Mod (GPa)	Shear Mod (GPa)
4130 Steel (Low Alloy Steel)	7850	460	280	200	80
Ni-Ti45 (Nitinol)	6.50E+03	450	150	60	24.8
Al 7068	2.85E+03	700	230	73	29
Banana Fiber	1.28E+03	730	10	28.5	4
Tungsten Carbide-Co-balt 84.02% WC	1.38E+04	3.20E+03	2.85E+03	540	220
Stainless Steel AM 355	7.77E+03	1.18E+03	570	205	78
Carbon Steel AISI 1080	7.80E+03	940	505	207.5	80

m1	Ranking m1	m2	Ranking m2	m3	Ranking m3	Average Rank
56.96988478	5	8.15287E+17	3	3.32909E+12	5	4.333333333
37.68445758	7	9.46215E+16	6	1.15385E+12	6	6.333333333
94.8017971	2	2.95088E+17	5	6.18713E+12	4	3.666666667
131.8901798	1	1.25E+16	7	26041666667	7	5
53.24977702	6	3.50725E+18	1	1.96196E+14	1	2.666666667
58.27146164	4	7.83012E+17	4	1.39382E+13	2	3.333333333
58.40021525	3	8.20513E+17	2	1.08985E+13	3	2.666666667

Table 10 - List of potential material candidates and their Respective rankings

'm_1', 'm_2' and 'm_3' respectively:

$$f(m_1) = \frac{E^{1/2}}{\rho}, \qquad f(m_2) = \frac{G^2}{\rho}, \qquad f(m_3) = \frac{\tau_{max}^{2/3}}{\rho}$$

Equation 4 - Merit indices for maximising mass for a specific stiffness, specific torsional stiffness and specific torsional strength

3.8.1 Derivation of m_1

Objective function:

$$\mathrm{m} = \pi \mathrm{r}^2 \mathrm{l} \mathrm{p}$$

Constraints:

- Length, *L* and Stiffness, *S**

Free Variables:

- Radius, *r*

Bending Equation:

$$\mathrm{S} = \frac{\mathrm{F}}{\delta}$$

Therefore:

$$\mathrm{S}^* = \frac{12\mathrm{E}\pi\mathrm{r}^4}{\mathrm{L}^3} \;\; \text{where } \mathrm{I} = \frac{\pi \mathrm{r}^4}{4} \text{ and } \delta = \frac{\mathrm{FL}^3}{48\mathrm{EI}}$$

Making r^2 the subject:

$$\mathrm{r}^2 = \frac{\sqrt{\mathrm{SL}^3}}{12\mathrm{E}\pi}$$

Substitution of r into the objective function:

$$\mathrm{m} = \mathrm{L}^{\frac{5}{2}} \times \frac{\sqrt{\pi}}{12} \times \mathrm{S}^{\frac{1}{2}} \times \frac{\rho}{\mathrm{E}^{\frac{1}{2}}}$$

Therefore, to minimise m, we need to maximise:

$$f(m_1) = \frac{E^{1/2}}{\rho}$$

3.8.2 Derivation of m_2

Objective function:

$$\mathrm{m} = \pi \mathrm{r}^2 \mathrm{l} \mathrm{p}$$

Constraints:

- Length, *L* and Stiffness, *S**

Free Variables:

- Radius, *r*

Torque Equation:

$$\frac{\tau}{\mathrm{r}} = \frac{\mathrm{T}}{\mathrm{r}} = \frac{\mathrm{G}\theta}{\mathrm{L}}$$

Which can be rearranged to:

$$\tau = \frac{\mathrm{T} \times \mathrm{r}}{\mathrm{I}} \text{ where } \mathrm{I} = \frac{\pi \mathrm{r}^4}{4}$$

Therefore:

$$r = (\frac{4\mathrm{M}}{\tau\pi})^{\frac{1}{3}}$$

Substitution of r into the objective function:

$$\mathrm{m} = \frac{\rho \mathrm{L}(4\mathrm{M})^{2/3}}{(\tau\pi)^{2/3}}$$

Therefore, to minimise m, we need to maximise:

$$f(m_2) = \frac{G^2}{\rho}$$

3.8.3 Derivation of m_3

Objective function:

$$\mathrm{m} = \pi \mathrm{r}^2 \mathrm{lp}$$

Constraints:

- Length, *L* and Stiffness, *S**

Free Variables:

- Radius, *r*

Bending Equation:

$$\frac{\tau}{\mathrm{r}} = \frac{\mathrm{M}}{\mathrm{I}} = \frac{\mathrm{E}}{\mathrm{R}}$$

Which can be rearranged to:

$$\mathrm{M} = \frac{\tau \mathrm{I}}{\mathrm{r}} \text{ where } \mathrm{I} = \frac{\pi \mathrm{r}^4}{4}$$

Therefore:

$$r = \frac{\sqrt[3]{4\mathrm{M}}}{\tau\pi}$$

Substitution of r into the objective function:

$$\mathrm{m} = \frac{\rho \mathrm{L}(4\mathrm{M})^{2/3}}{\tau^{2/3}}$$

Therefore, to minimise m, we need to maximise:

$$f(m_3) = \frac{\tau_{max}^{2/3}}{\rho}$$

The material with the highest average rank was Stainless Steel AM 355, however Al 7068 was chosen for the final design as it met the design requirements and cost significantly less to manufacture.

Aluminium alloys have significantly lower specific energy than stainless steels. The specific energy of a materials refers to energy needed to process the material which is shown in *Table* 12. Aluminium's lower specific energy means less energy is required for extraction, refinement and shaping.

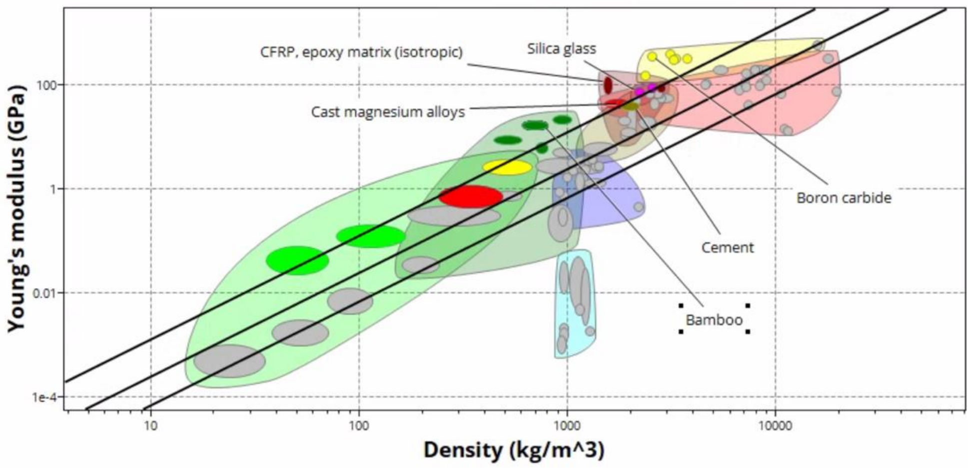

Figure 31 - Ashby Chart for Specific Stiffness

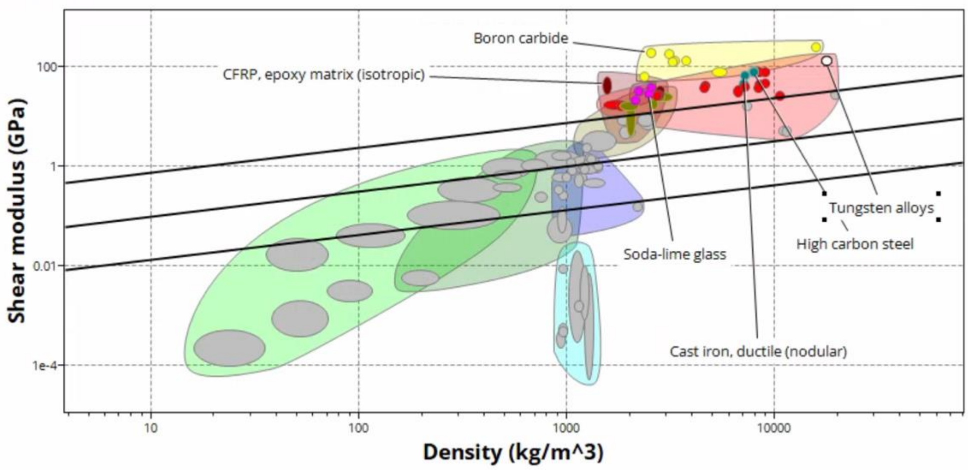

Figure 32 - Ashby Chart for Specific Torsional Stiffness

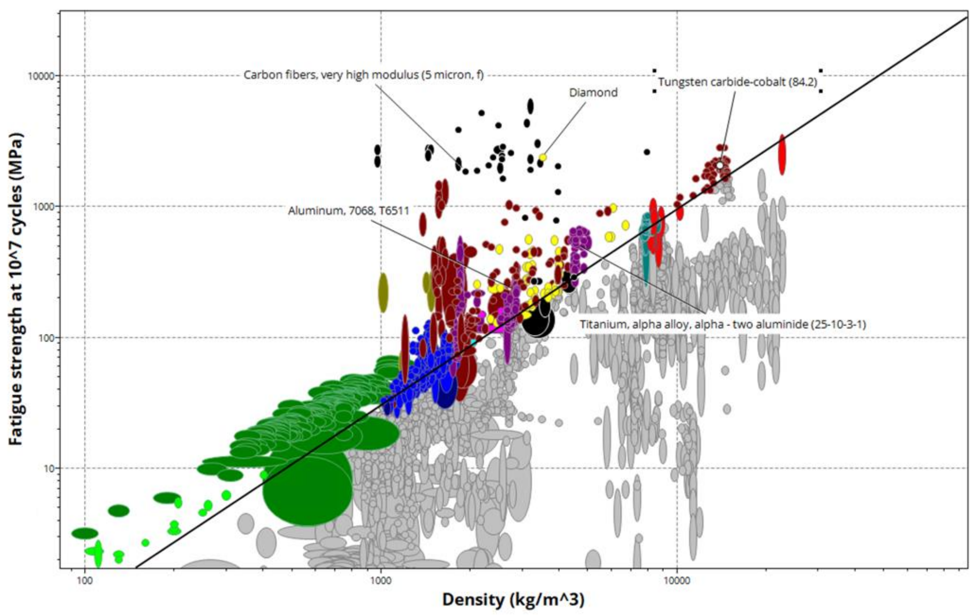

Figure 33 - Ashby Chart for Specific Torsional Strength

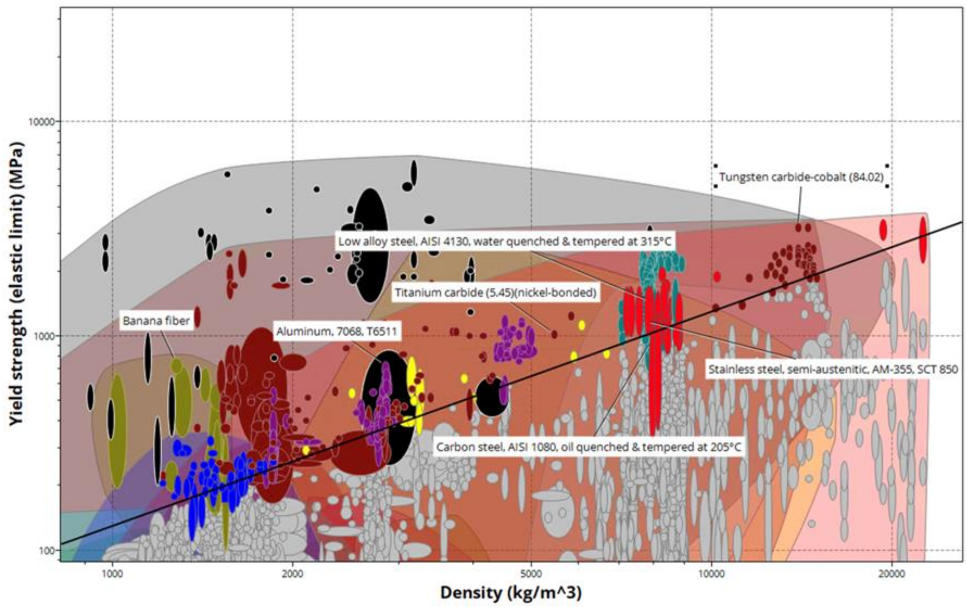

Figure 34: The Ashby chart for yield strength against density of materials. An initial screening of materials represented by the black separates the minimum strength to density ratio desired. On the graph, the seven selected materials have been identified using arrows.

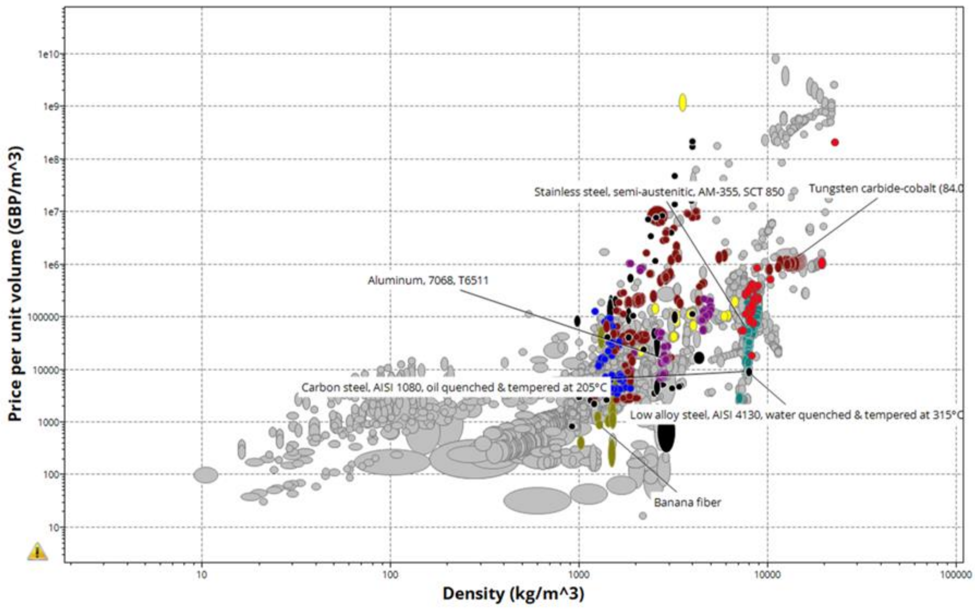

Figure 35: A second screening of materials based on their price per unit volume to density ratio. The Ashby chart once again identifies the seven selected materials.

3.8.4 Secondary Constraints

The following points consider the secondary constraint trade-offs involved with choosing Al 7068.

- Corrosion Resistance
  - Al 7068 has lower corrosion resistance compared to other aluminium alloys due to its high zinc content.
- Cost
  - Al 7068 is among the most expensive aluminium alloys due to its high-performance characteristics.
- Fatigue Resistance
  - Al 7068 has excellent fatigue resistance.

3.8.5 Material Conclusion

This material was selected qualitatively and quantitatively based on the following criteria:

- Merit indices for
  - specific stiffness
  - specific torsional stiffness
  - specific torsional strength
- Price
- Yield strength
- Density
- Secondary Constraints
  - Corrosion resistance
  - Cost
  - Fatigue resistance
- Carbon footprint
  - Energy consumption requirements for manufacturing dictate that aluminium is more efficient due than steels, to its lower specific energy as well as its lightweight properties, minimising operational energy consumption during its lifecycle

3.9 Manufacturing Considerations

The main manufacturing method is turning. Five calculations were made for the five sections of the shaft.

The Material Removal Rate was calculated from:

$$MMR = \pi \times D_{avg} \times d \times V_{axial}$$

Equation 5 - Material Removal Rate Equation

The machining time was calculated by multiplying volume to be removed by material removal rate:

$$T_m = V \times MMR$$

Equation 6 - Machining Time Equation

The machining power was calculated by multiplying the material removal rate by the specific energy of the material:

$$P_m = MMR \times U$$

Equation 7 - Power Required Equation

The energy required was calculated by multiplying power required by time:

$$E = P_m \times T_{mT}$$

Equation 8 - Energy Required Equation

The maximum cutting force was calculated by dividing the machining power by the cutting speed:

$$F_c = \frac{P_m}{V}$$

Equation 9 - Maximum Cutting Force Equation

From this, the resultant force can then be calculated:

$$R = \frac{F_c \tan(\beta - \alpha)}{\sin(\beta - \alpha)}$$

The machining cost was calculated by multiplying the total time in seconds by the labour cost plus burden rate using:

$$C_m = \frac{T_{mT}}{3600} \times (L_m + B_m)$$

Equation 10 - Total Cost for the machining of the Shaft

Assuming an hourly wage of £10/hour, with an overhead of £4/hour the labour cost rate amounts to £14/hour.

Below are the corresponding tabulated values, using the forementioned equations:

Summary of Turning Parameters							
Parameter	**Symbol**	**Unit**	**Value**				
Shear Angle	ϕ	°	36				
Rake Angle	α	°	12				
Friction Angle	β	°	30				
Rotational Speed of the Workpiece	N	rpm	420				
Feed	f	mm/rev	0.523809524				
Linear Tool Speed Along Workpiece	v	mm/min	220				
Workpiece Surface Speed	V	m/s	1.374446786	1.429424657	1.5393804	1.429424657	1.37444679
Length of Cut	l	mm	30	180	600	200	100
Stock Diameter	D0	mm	70	70	70	70	70
Diameter	Df	mm	55	60	70	60	55
Average Diameter	Davg	mm	62.5	65	70	65	62.5
Maximum Cut Depth	d	mm	4	4	4	4	4
Material Removal Rate	MRR	mm^3/s	2879.793266	2994.984996	3225.368458	2994.984996	2879.79327
Total Stock Volume	V	mm^3	115453.53	692721.1801	2309070.6	769690.2001	384845.1
Total Shaft Section Volume	V	mm^3	71274.88333	508938.0099	2309070.6	565486.6776	237582.944
Total Material to be Removed	V	mm^3	44178.64669	183783.1702	0	204203.5225	147262.156
Time	T	s	15.34090909	61.36363636	0	68.18181818	51.1363636
Power Required	P	W	2879.793266	2994.984996	3225.368458	2994.984996	2879.79327
Energy Required	E	J	44178.64669	183783.1702	0	204203.5225	147262.156
Cutting Force	Fc	N	2095.238095	2095.238095	2095.238095	2095.238095	2095.2381
Torque Required for Cutting	T	Nm	65476.19048	68095.2381	73333.33333	68095.2381	65476.1905
Reaction Force	R	N	2203.063708	2203.063708	2203.063708	2203.063708	2203.06371
Labour Cost Rate	Lm	£/hour	14	14	14	14	14
Burden Rate	Bm	£/hour	53.41592632	53.68161402	54.19808186	53.68161402	53.4159263
Machining Cost	Cm	£	0.287283777	1.153663875	0	1.28184875	0.95761259
Total Machining Cost	Cmt	£	3.680408993				

Table 11 - Manufacturing Calculations

Material Specific Energy	
Material	**Specific Energy (W s/mm^3)**
Aluminium alloys	0.4 - 1.0
Cast irons	1.1 - 5.4
Copper alloys	1.4 - 3.2
High-temperature alloys	3.2 - 2.8
Magnesium alloys	0.3 - 0.6
Nickel alloys	4.8 - 6.7
Refactory alloys	3.0 - 9.0
Stainless steels	2.0 - 5.0
Steels	2.0 - 9.0
Titanium alloys	2.0 - 5.0
Chosen Material	1

Table 12 - Specific Energy of Materials

The Total Machining cost C_m was the sum of machining costs and was £3.68.

To meet the power requirements from *Table 11*, the 5 kW lathe is used for turning operations.

Machining costs increase with improvements in surface quality as depicted in the following graph:

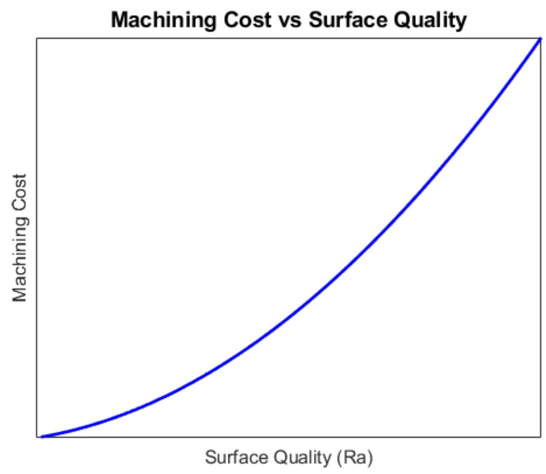

Figure 36 – Qualitative graph representing the relationship between surface quality and machining cost. Machining cost increases for a higher surface quality due to the need for greater precision and better tools.

The following machining processes were used for manufacturing the shaft:

- Turning
    - Reducing shaft cross section
    - Chamfers
    - Shoulders
    - Parting
    - Circlip grooves
- Vertical Milling
    - Key seats

Appendix A: Initial Calculations

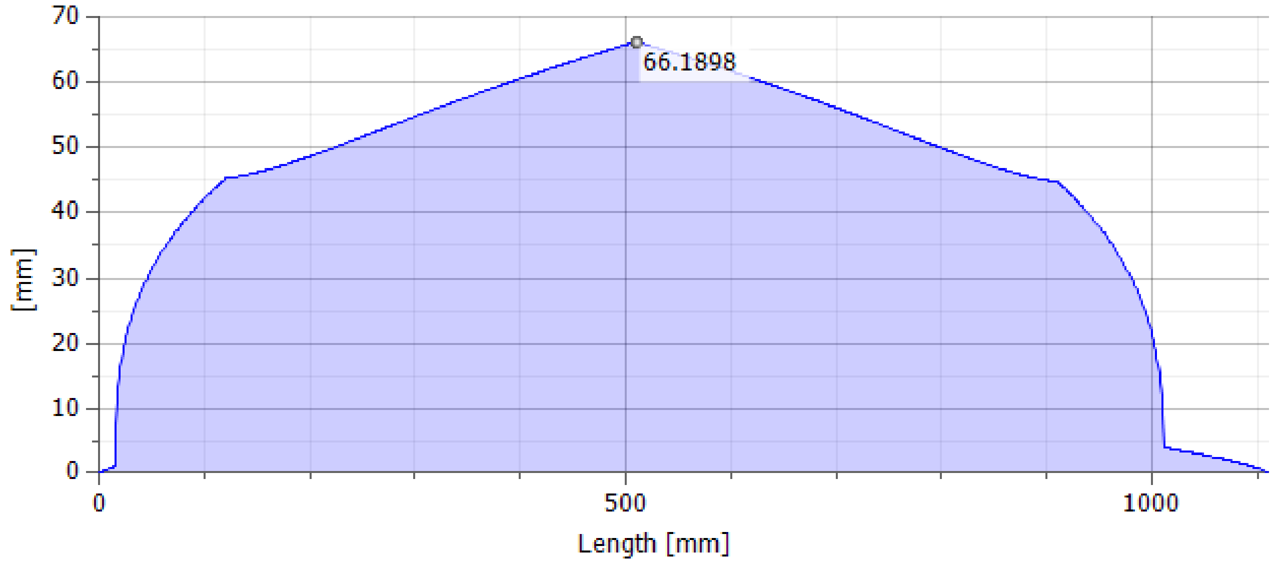

Ideal diameter along the length of the shaft.

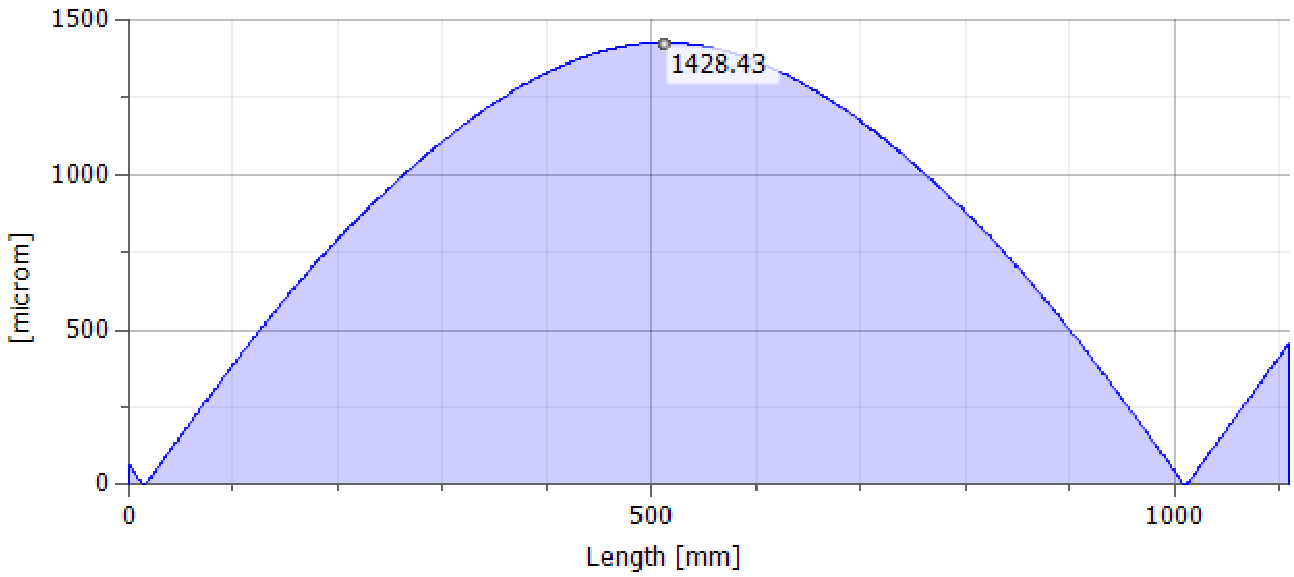

Combined Deflection along length of the shaft

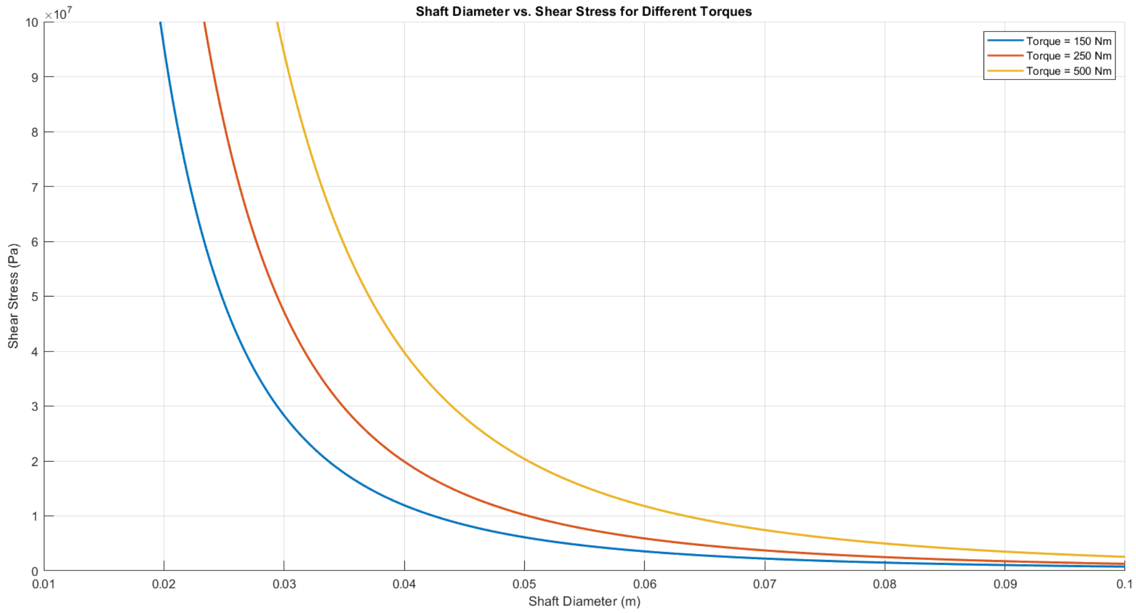

Ideal diameter along length of the shaft based on the torque applied on the shaft for the Al 7068 material.

Appendix B: Power Transmission

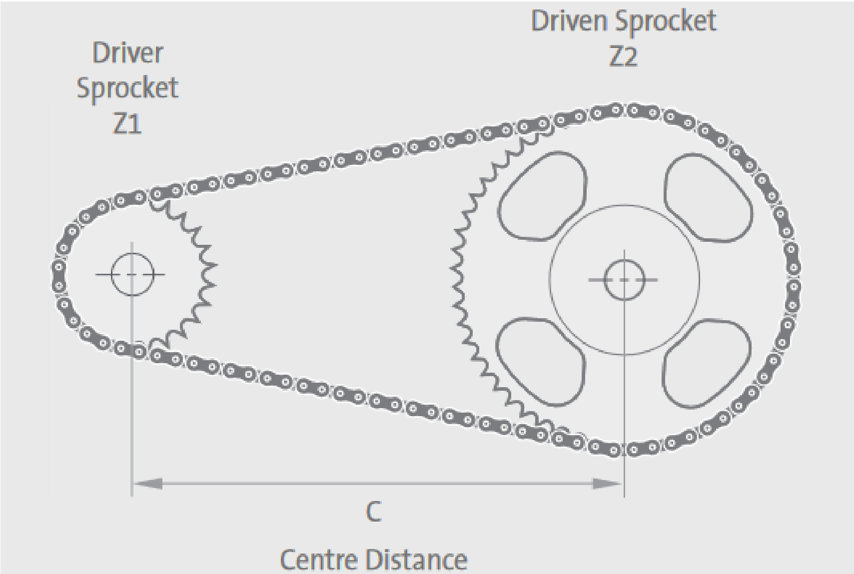

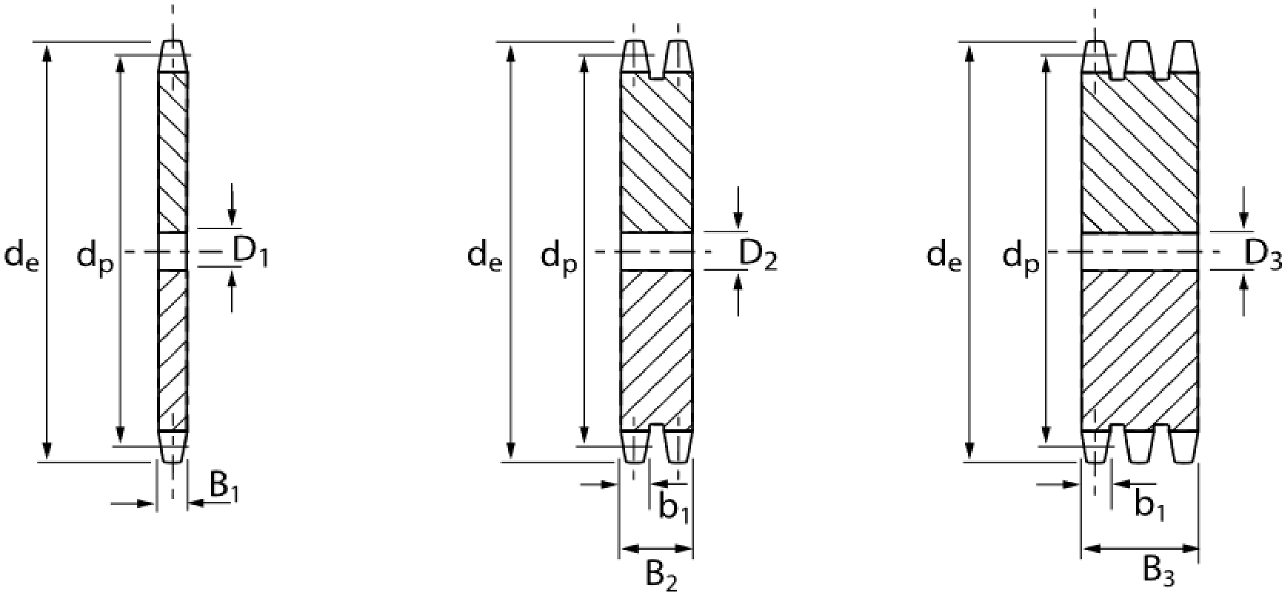

Sprocket Dimensions

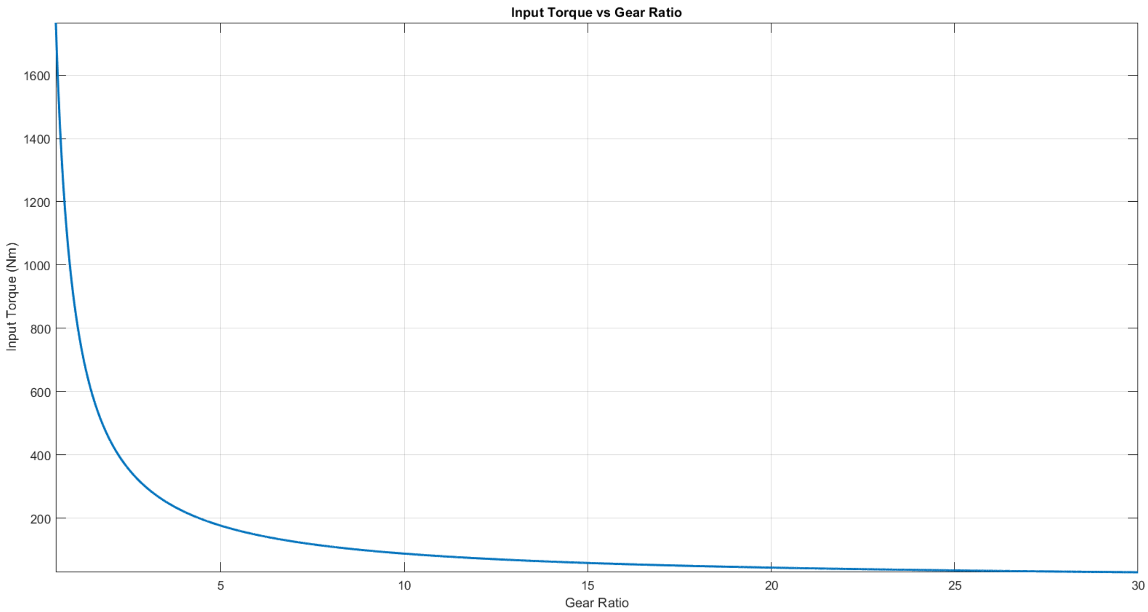

Relationship between input torque and gear ratio for the required output torque

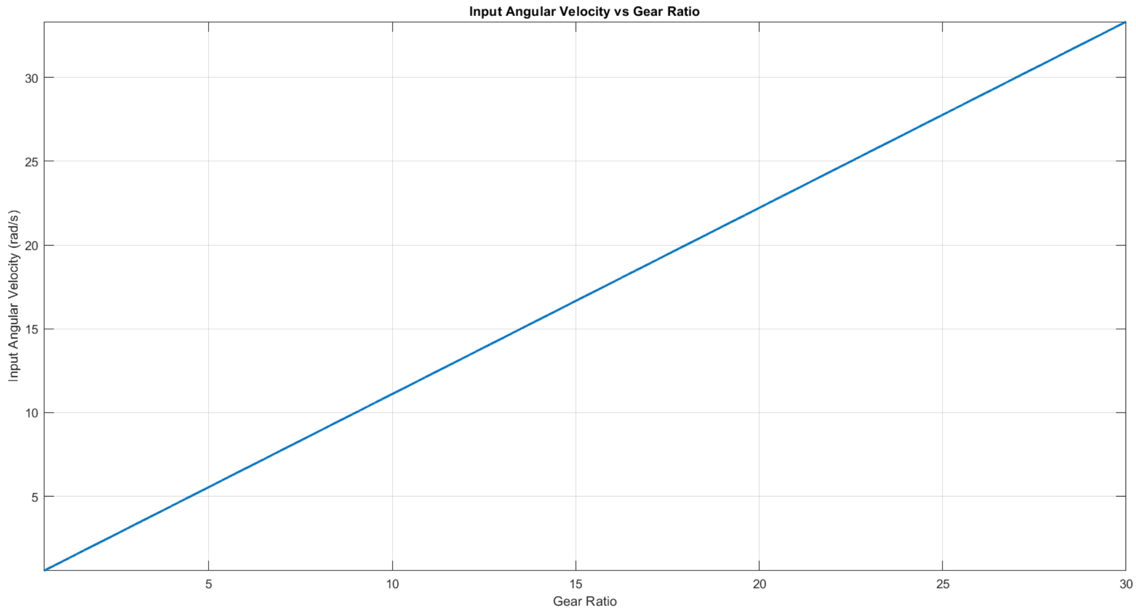

Relationship between input angular velocity and gear ratio to achieve the required output angular velocity.

Appendix C: Auxiliary Components

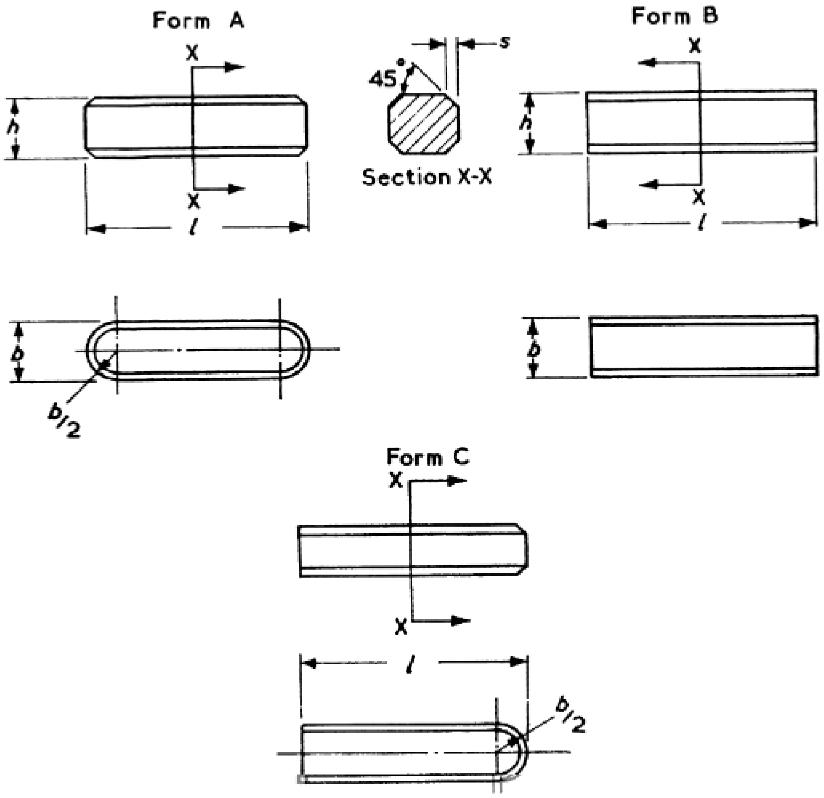

Key dimensions

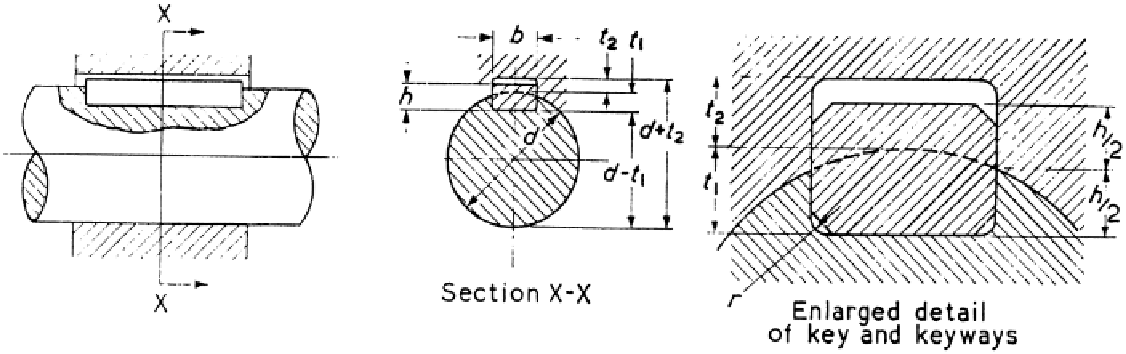

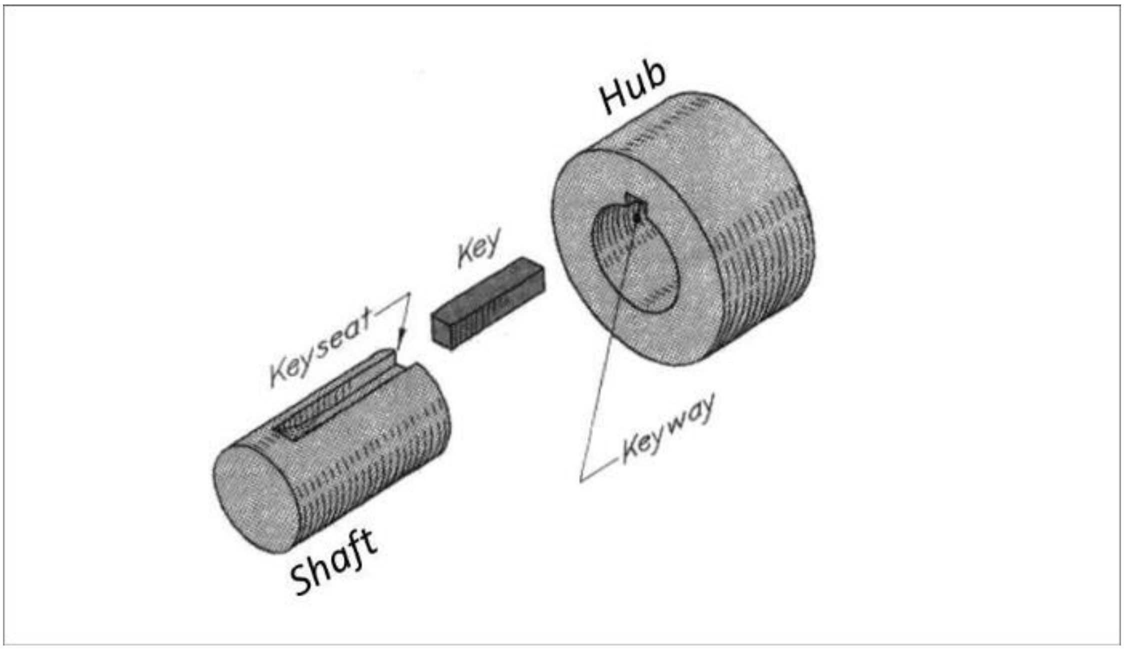

Single row deep groove ball bearing

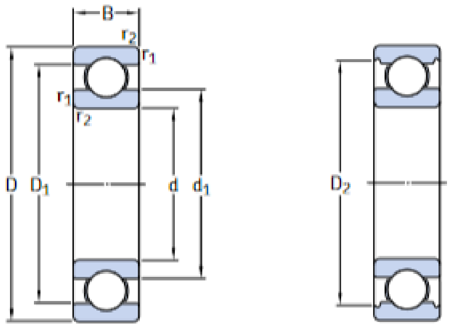

Bearing dimensions

Appendix D: Manufacturing